Dual-Polarized IRS-Enhanced Generalized Multiuser Multi-Stream MIMO

Muteen Munawar, Mamoun Guenach, and Ingrid Moerman, *Senior Member, IEEE*

***Abstract*—This paper investigates a dual-polarized intelligent reflecting surface (DP-IRS)-assisted multiuser multiple-input multiple-output (MIMO) wireless network with the possibility of multi-stream transmission per user. We aim to determine the number of data streams per user while simultaneously ensuring that each user achieves its specified target spectral efficiency performance with the minimum transmit power. To achieve this, we optimize the number of data streams, power allocations, transmit/receive digital filters, DP-IRS operations, and transmit/receive DP antennas phase shifters. Based on this generalized network setup, we formulate an optimization framework involving multiple coupled optimization variables. To tackle this complex optimization problem, we first derive low-complexity convex formulations for each variable. Subsequently, we propose a novel multi-step alternating optimization algorithm that effectively solves multiple subproblems sequentially and converges to a feasible solution. Motivated by further complexity reduction, we present a low-complexity suboptimal version of the main algorithm. Extensive numerical simulations demonstrate that, compared to a simple IRS, the DP-IRS achieves a 42.4% reduction in transmit power for a configuration with 50 reflecting elements and eight users. Additionally, the proposed low-complexity Algorithm 2 incurs a 62% decrease in computational complexity compared to Algorithm 1 while maintaining satisfactory performance.**

***Index Terms*—Intelligent reflecting surface, dual polarization, multi-user, multiple-input multiple-output, multi-stream transmission, alternating optimization.**

I. Introduction

Recent developments in metamaterials have made it possible to control metamaterial properties in real time. This opens up new opportunities for using metasurfaces in wireless communication [1]. Different types of metasurfaces have been proposed in antenna and electromagnetic literature with promising performance and applications in wireless communications. For example, a metasurface-based simple intelligent reflecting surface (S-IRS) [2] can provide real-time amplitude and phase changes to the incident signal, offering potential applications such as improved signal-to-noise ratio (SNR) [3], enhanced coverage [4], increased security [5], reduced interference [6], and reflected modulation [7]. Corresponding to these applications, a wealth of literature exists on beamforming and channel estimation methods for S-IRS [8]–[10]. Other metasurfaces, such as simultaneous transmit and reflecting-IRS [11], omni-intelligent surface [12], and active-IRS [13], also exhibit unique features and potential capabilities for use in wireless communication networks.

While an extensive body of literature has delved into the applications of S-IRS [14], this study uniquely centers on the realm of dual-polarized IRS-assisted wireless networks. A dual-polarized IRS (DP-IRS), considered in this paper [15]–[17], represents a metasurface endowed not only with amplitude and phase changing capabilities but also with the ability to perform polarization beam splitting, polarization conversion, and the independent control of split beams. The precise manipulation of these functionalities, coupled with the inherent traits of polarization diversity, polarization multiplexing, and passive polarization modulation, opens up a plethora of potential applications for wireless communication systems.

Despite the extensive exploration of dual-polarized metasurfaces in the electromagnetic and antenna design domains, as evidenced in works such as [15]–[17], and considering the prevalence of modern communication systems operating on dual-polarization waves, their applications in wireless communication remain largely untapped.

A. Literature on DP-IRS:

A conventional DP-IRS with two components per element, namely vertical and horizontal, is considered in [18]. This study proposes performing reflect modulation using two parallel orthogonal passive data streams. More specifically, it considers a scenario where a single transmitting antenna acts as the source of radio signals, and these signals, upon impinging on the DP-IRS, are manipulated to emulate a QAM modulation symbol for information modulation. Thus, the multiple elements of the DP-IRS and multiple receiving antennas create a MIMO-like scenario.

In [19], authors also examine a similar DP-IRS with two components per element, namely vertical and horizontal, which are designed to respond to the corresponding polarization for amplitude and phase shift control. The focus of this paper is limited to broadbeam applications. Specifically, the authors aim to leverage the dual polarization capabilities of the DP-IRS to provide a uniform SNR across multiple users in the system, rather than focusing on Signal-to-Interference-plus-Noise Ratio (SINR) enhancements as in our scenario. This application is particularly beneficial for transmissions common to all users, such as those found in broadbeam scenarios, and is limited to enhancing SNR rather than addressing SINR improvements. In [20]–[22], the authors again

The research leading to these results has received funding from the European Community's Research Foundation Flanders (FWO) under grant agreement no A2582˙00˙01˙01, Project Strip-link MIMO FWO - 97707, and IMEC ARF Program 97700/01345. (Corresponding author: Muteen Munawar.)

Muteen Munawar, Mamoun Guenach, and Ingrid Moerman are affiliated with the Interuniversity Microelectronics Centre (IMEC), Leuven, Belgium, the Internet Technology and Data Science Lab (IDLab) research group at Ghent University, Ghent, Belgium, and Ghent University, Ghent 9050, Belgium, respectively. (e-mail: Muteen.Munawar@imec.be).

study DP-IRS, a traditional extension from single polarization to dual-polarization, and depict the explicit dual polarization multiplexing gains. They treat the two polarizations as two orthogonal, parallel S-IRS systems, meaning no new algorithms are required. More specifically, [22] focuses on the electromagnetic radiation behaviors of vertically and horizontally reflected signals in a DP-IRS, and considers a scenario with two users, i.e., one user per polarization, to depict the explicit multiplexing gains.

The most closely related DP-IRS, i.e., one with beam splitting and polarization conversion properties, is studied in [23], [24] and [25]. In these works, DP-IRS is employed in a non-orthogonal multiple access system to mitigate interference and address depolarization concerns, respectively.

B. Contribution

Building upon the earlier work in [24], which aimed to harness the interlayer multiplexing of DP-IRS without relying on the explicit multiplexing gains of DP waves and was limited to a single-user DP-IRS-assisted network, this paper extends that work to address a more complex and generalized wireless system. In this extended study, a DP-IRS collaborates with a multi-antenna transmitter to communicate with multiple users, each equipped with multiple antennas, thereby enabling the transmission of multiple data streams to each user. The primary objective is to optimize the number of data streams for each user, to achieve the targeted spectral efficiency (SE) performance with the minimum transmit power at the transmitter. To the best of our knowledge, this is the first study on the aforementioned DP-IRS-aided multi-stream transmission per user, coupled with a single RF chain per DP antenna, to observe interlayer multiplexing gains.

To achieve this goal, we formulate a complex optimization problem with multiple interconnected variables, including the number of data streams per user, power allocations, digital precoder/combiners, DP-IRS operations, and phase shifters for transmit/receive DP antennas. Notably, the system considered here lacks inherent explicit polarization multiplexing (PM) gains due to the presence of a single RF chain per DP antenna. However, we leverage the unique capabilities of DP-IRS to attain implicit PM gains, coupled with polarization diversity gains, thereby enhancing inter-layer multiplexing. The main contributions of our study can be summarized as follows:

- We derive low-complexity convex formulations for various parameters, including the number of data streams per user, power allocations, digital precoder/combiners, DP-IRS operations, and phase shifters for transmit/receive DP antennas. Leveraging these formulations, we propose a novel multistep alternating optimization (AO) algorithm designed to systematically address these convex formulations until convergence is achieved. The convex formulations, coupled with the proposed algorithm, are specifically crafted to uphold monotonic behavior in the objective value, thereby guaranteeing the algorithm's convergence to a viable solution.
- By relaxing the optimization of the number of data streams per user and their corresponding weights, we introduce Algorithm 2, which exhibits lower computational complexity at the expense of performance degradation.
- Finally, we present an extensive numerical analysis and discussions for the proposed algorithms, considering several benchmark schemes for a comprehensive evaluation. we also discuss the extension of this work to address the problem of sum capacity maximization.

The remainder of this paper is organized as follows. Section II discusses the system model and formulates the problem. The proposed algorithms are presented in Sections III and IV. In Section V, we numerically evaluate the performance of the proposed algorithms and compare them with benchmark schemes. Finally, Section VI concludes the paper.

Notations: Scalars are denoted by italic letters, whereas vectors and matrices are denoted by bold-face lower- and upper-case letters, respectively. The subscripts/superscripts v and h denote vertical and horizontal polarization, respectively. For a complex-valued vector $\mathbf{v}$ of length N, $\mathbf{v}^T$ denotes the transpose, $v_{(n)}$/$\mathbf{v}_{(n)}$ denotes the nth element of $\mathbf{v}$, $\mathbf{v}^*$ denotes the complex conjugate of each element, $\mathbf{1}_{\mathbf{v}}$ denotes a vector of size $\mathbf{v}$ with all entries 1, $\mathbf{v}^H$ denotes the conjugate transpose, $\|\mathbf{v}\|$ denotes the Euclidean norm, $\mathrm{diag}\,(\mathbf{v})$ denotes a diagonal matrix with each diagonal element being the corresponding element in $\mathbf{v}$, $\arg(\mathbf{v})$ denotes a vector with each element being the phase of the corresponding element in $\mathbf{v}$, $\mathbf{v} > 0$ denotes the number of non zero elements in $\mathbf{v}$, $\mathrm{logsum}\,(\mathbf{v})$ means $\sum_{k=1}^{K} \log(\mathbf{v}_k)$, $\mathrm{sum}\,(\mathbf{v})$ means $\sum_{k=1}^{K} (\mathbf{v}_k)$, and $\mathrm{GM}\,(\mathbf{v})$ represents the geometric mean. For a complex-valued matrix $\mathbf{M}$, $\mathrm{rank}\,(\mathbf{M})$ denotes the rank, $\mathbf{M}_{(n,m)}$ denotes the n-th row and m-th column entry, $\|\mathbf{M}\|_F$ denotes Frobenius norm, $\mathbf{M} \succeq 0$ denotes positive semi-definite, $\mathbf{M} \circ \mathbf{M}$ denotes the Hadamard product, and $\mathrm{trace}\,(\mathbf{M})$ denotes trace. For a complex-valued square matrix $\mathbf{A}$, $\mathbf{I}_{\mathbf{A}}$ denotes an identity matrix of size $\mathbf{A}$ and $\mathbf{A}^{-1}$ denotes the inverse. The notation $(\cdot)^*$ denotes the complex conjugate of a complex number, $\hat{e}_{\max}(\mathbf{A}, \mathbf{B})$ denotes the dominant generalized eigenvector of matrix pair $(\mathbf{A}, \mathbf{B})$, and $f()$ denotes the function.

II. System Model

Fig. 1 depicts the generalized multiuser MIMO communication system where a DP-IRS with N reflecting elements assists an access point (AP) with N_t transmit DP antennas to communicate with K number of receivers, each with $N_{r,k}$ receive DP antennas and L_k number of data streams resulting in the total $L = \sum_{k=1}^{K} L_k$ data streams in the system, where $k = 1, \ldots, K$. For clarity and in order to establish the signal model, let's consider the case where $N_t = K = N_{r,k} = 1$. The received signal in this scenario can be expressed as:

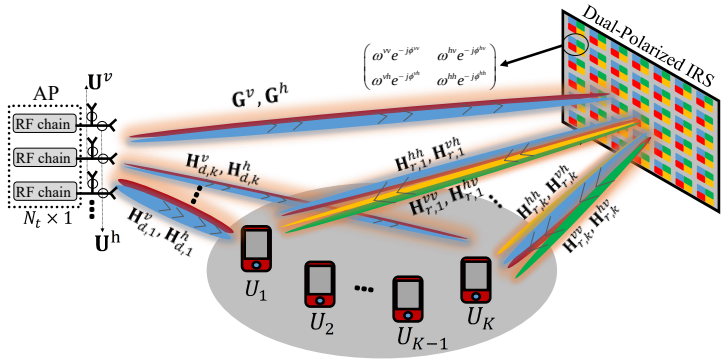

Fig. 1: System model.

$$\begin{bmatrix} y^v \\ y^h \end{bmatrix} = f \begin{pmatrix} e^{-j\delta^v} & 0 \\ 0 & e^{-j\delta^h} \end{pmatrix} \Bigg[\Bigg\{ \begin{pmatrix} (h_r^{vv})^* & (h_r^{hv})^* \\ (h_r^{vh})^* & (h_r^{hh})^* \end{pmatrix} \circ \underbrace{\begin{pmatrix} \omega^{vv} e^{-j\phi^{vv}} & \omega^{vh} e^{-j\phi^{vh}} \\ \omega^{hv} e^{-j\phi^{hv}} & \omega^{hh} e^{-j\phi^{hh}} \end{pmatrix}}_{\mathbf{\Psi}} \circ \begin{pmatrix} g^{vv} & g^{hv} \\ g^{vh} & g^{hh} \end{pmatrix} + \begin{pmatrix} (h_d^v)^* & 0 \\ 0 & (h_d^h)^* \end{pmatrix} \Bigg\}^T \begin{pmatrix} e^{-j\gamma^v} & 0 \\ 0 & e^{-j\gamma^h} \end{pmatrix} \sqrt{\frac{P_t}{2}} w \Bigg]^T \mathbf{s}, \tag{1}$$

where y^v, y^h, f, $(h_r)^*$, $(h_d)^*$, $\mathbf{\Psi}$, g, $\mathbf{s}$, P_t and w represent the received vertical polarized signal, received horizontal polarized signal, receive digital filter, IRS-user channel, AP-user channel, reflecting element operation, AP-IRS channel, transmitted symbol, transmit power, and transmit digital filter, respectively. In $\mathbf{s}$, the entries are the same, indicating that the same information symbol is transmitted to both radiation patches. Within the $\mathbf{\Psi}$ matrix, the variables ω and ϕ denote the amplitude and phase changes of the reflected signal. Notably, subscripts pq indicate polarization conversion from p to q, where $p, q \in v, h$. The matrices $\mathrm{diag}(e^{-j\delta^v}, e^{-j\delta^h})$ and $\mathrm{diag}(e^{-j\gamma^v}, e^{-j\gamma^h})$ in (1) represent the transmit phase shifters at the AP and receive phase shifters at the user, respectively. Given the constraint of a single RF chain, the total transmission power P_t in (1) is uniformly distributed between the two radiated polarizations, specifically as $\sqrt{\frac{P_t}{2}} w$. In (1), both f and w act as common digital filters for both polarizations; nevertheless, when combined with the transmit-receive DP antennas' phase shifts, they result in distinct hybrid filters. The significance of such hybrid DP antennas is prominent in subsequent sections, where the model is extended to the MIMO scenario. More details on (1) and DP antennas can be found in [23], [24] and [26], [27], respectively. The signal model provided in (1) can be readily extended to include N_t transmit antennas, N reflecting elements, and K users, yielding (2):

$$\begin{aligned} \mathbf{y}_k &= \mathbf{y}_k^v + \mathbf{y}_k^h \\ &= \mathbf{F}_k \Big(\mathbf{E}_k^v \Big\{ \left(\mathbf{H}_{r,k}^{vv}\right)^H \mathbf{\Phi}^{vv} \mathbf{G}^{vv} + \left(\mathbf{H}_{r,k}^{hv}\right)^H \mathbf{\Phi}^{vh} \mathbf{G}^{hv} \\ &\quad + \left(\mathbf{H}_{d,k}^{v}\right)^H \Big\} \mathbf{U}^v + \mathbf{E}_k^h \Big\{ \left(\mathbf{H}_{r,k}^{vh}\right)^H \mathbf{\Phi}^{hv} \mathbf{G}^{vh} + \left(\mathbf{H}_{r,k}^{hh}\right)^H \\ &\quad \cdot \mathbf{\Phi}^{hh} \mathbf{G}^{hh} + \left(\mathbf{H}_{d,k}^{h}\right)^H \Big\} \mathbf{U}^h \Big) \cdot \sum_{j=1}^{K} \sum_{l=1}^{L_j} \mathbf{w}_{j,l} s_{j,l} + \mathbf{F}_k \mathbf{z}_k, \end{aligned} \tag{2}$$

where $\{\mathbf{y}_k^v, \mathbf{y}_k^h\} \in \mathbb{C}^{N_{r,k} \times 1}$, $\mathbf{F}_k \in \mathbb{C}^{L_k \times N_{r,k}}$, $\left[\mathbf{w}_{k,1}, \mathbf{w}_{k,2}, \cdots, \mathbf{w}_{k,L_j}\right]$, and $\mathbf{z}_k$, represent receive vertical/horizontal signal, receive digital filter, transmit digital filter, and noise vector for user k, respectively, whereas $\mathbf{w}_{j,l} \in \mathbb{C}^{N_t \times 1}$ is the transmit digital filter for the l-th data stream of j-th user and $s_{j,l}$ is the data symbol sent over the lth data stream of the jth user with $\{k, j\} = 1, \cdots, K$, $l = 1, \cdots, L_k$. The matrices $\mathbf{U}^v \in \mathbb{C}^{N_t \times N_t}$, $\mathbf{U}^h \in \mathbb{C}^{N_t \times N_t}$, $\mathbf{E}_k^v \in \mathbb{C}^{N_{r,k} \times N_{r,k}}$, and $\mathbf{E}_k^h \in \mathbb{C}^{N_{r,k} \times N_{r,k}}$ contain the transmit vertical phase shifters, transmit horizontal phase shifters, receive vertical phase shifters, and receive horizontal phase shifters in the diagonal, i.e., $\mathbf{U}^p = \mathrm{diag}(e^{-j\gamma_{p,1}}, e^{-j\gamma_{p,2}}, e^{-j\gamma_{p,3}}, \cdots, e^{-j\gamma_{p,N_t}})$ and $\mathbf{E}_k^p = \mathrm{diag}(e^{-j\delta_{p,1}}, e^{-j\delta_{p,2}}, e^{-j\delta_{p,3}}, \cdots, e^{-j\delta_{p,N_{r,k}}})$, where $p \in \{v, h\}$. The baseband equivalent channels for user k are denoted by $\mathbf{G}^{pq} \in \mathbb{C}^{N \times N_t}$, $(\mathbf{H}_{r,k}^{pq})^H \in \mathbb{C}^{N_{r,k} \times N}$, and $(\mathbf{H}_{d,k}^{p})^H \in \mathbb{C}^{N_{r,k} \times N_t}$ for AP-IRS, IRS-User, and AP-User links, respectively.

Considering the proximity of each component within a reflective element, a reasonable assumption is that the channels between analogous polarizations in both the AP-IRS and IRS-user links are identical [28]. The simplified aggregate received signal at user k can be represented as (3). Let

TABLE I: Notation Description

Notation	Description
N	Number of reflecting elements.
N_t	Number of transmit antennas.
$N_{r,k}$	Number of receive antennas at user k.
K	Total number of users.
L_k	Number of data streams for user k.
$\mathbf{f}_{k,l}^H \in \mathbb{C}^{1 \times N_{r,k}}$	Receive digital filter for the lth data stream of user k.
$\mathbf{w}_{k,l} \in \mathbb{C}^{N_t \times 1}$	Transmit digital filter for the lth data stream of user k.
$\mathbf{E}_k^p \in \mathbb{C}^{N_{r,k} \times N_{r,k}}$	Diagonal matrix containing the kth user's receive DP antenna phase shifters for polarization p, where $p \in \{v, h\}$.
$\mathbf{U}^p \in \mathbb{C}^{N_t \times N_t}$	Diagonal matrix containing transmit DP antenna phase shifters for polarization p, where $p \in \{v, h\}$.
$\mathbf{\Phi}^{pq} \in \mathbb{C}^{N \times N}$	Diagonal matrix containing DP-IRS operations for the pq subpart, where $p, q \in \{v, h\}$.
$\left(\mathbf{H}_{d,k}^{p}\right)^H \in \mathbb{C}^{N_{r,k} \times N_t}$	Direct channel between polarization p of the AP and polarization p of user k.
$\left(\mathbf{H}_{r,k}^{pq}\right)^H \in \mathbb{C}^{N_{r,k} \times N}$	Channel between the pq part of the DP-IRS and polarization q of user k.
$\mathbf{G}^{pq} \in \mathbb{C}^{N \times N_t}$	Channel between polarization p of the AP and the pq part of the DP-IRS.
$\rho_{k,l}$	Power allocated to the lth data stream of user k.
p_k	Power allocated to user k such that $p_k = \sum_{l=1}^{L_k} \rho_{k,l}$.
$P_{\max}$	Maximum transmit power budget at the AP.
$o_{\mathbf{x}}^k$	Auxiliary variable for user k treated as part of the objective function in the optimization of x.
y_{kl}	Auxiliary variable treated as an optimal weight for the lth data stream of user k.
$\hat{e}_{\max}(\mathbf{A}, \mathbf{B})$	Dominant generalized eigenvector of matrix pair $(\mathbf{A}, \mathbf{B})$.

$\mathbf{H}_k^H = (\mathbf{E}_k^v\{(\mathbf{H}_{r,k}^v)^H(\mathbf{\Phi}^{vv}\mathbf{G}^v + \mathbf{\Phi}^{vh}\mathbf{G}^h) + (\mathbf{H}_{d,k}^v)^H\}\mathbf{U}^v) + (\mathbf{E}_k^h\{(\mathbf{H}_{r,k}^h)^H(\mathbf{\Phi}^{hv}\mathbf{G}^h + \mathbf{\Phi}^{hh}\mathbf{G}^h) + (\mathbf{H}_{d,k}^h)^H\}\mathbf{U}^h)$ denotes the composite channel between the AP and user k, the SE for user k provided by L_k data streams , i.e, c_k, is given by (4), where $\mathbf{f}_{k,l}$ is the receive digital filter for the l-th data stream of k-th user, such that $\mathbf{F}_k^H = \left[\mathbf{f}_{k,1}, \mathbf{f}_{k,2}, \cdots, \mathbf{f}_{k,L_k}\right]$. Additional information regarding the system model, channel models, and DP-IRS operations can be found in [15]–[17], [24]–[26], [28]. Due to brevity and to prevent redundancy with existing literature, these details are omitted here.

$$\mathbf{y}_k = \mathbf{F}_k\Big(\mathbf{E}_k^v\Big\{\left(\mathbf{H}_{r,k}^v\right)^H\left(\mathbf{\Phi}^{vv}\mathbf{G}^v + \mathbf{\Phi}^{vh}\mathbf{G}^h\right) + \left(\mathbf{H}_{d,k}^v\right)^H\Big\} \cdot \mathbf{U}^v + \mathbf{E}_k^h\Big\{\left(\mathbf{H}_{r,k}^h\right)^H\left(\mathbf{\Phi}^{hh}\mathbf{G}^h + \mathbf{\Phi}^{hv}\mathbf{G}^v\right) + \left(\mathbf{H}_{d,k}^h\right)^H\Big\} \cdot \mathbf{U}^h\Big) \cdot \sum_{j=1}^{K}\sum_{l=1}^{L_j}\mathbf{w}_{j,l}s_{j,l} + \mathbf{F}_k\mathbf{z}_k. \tag{3}$$

$$\begin{aligned} c_k &= f\left(\mathbf{W}, \mathbf{F}_k, L_k, \mathbf{U}^p, \mathbf{\Phi}^{pq}, \mathbf{E}_k^p\right) \\ &= \sum_{l=1}^{L_k}\log_2\left(1 + \frac{\left|\mathbf{f}_{k,l}\mathbf{H}_k^H\mathbf{w}_{k,l}\right|^2}{\sum\limits_{j\neq l}^{L_k}\left|\mathbf{f}_{k,l}\mathbf{H}_k^H\mathbf{w}_{k,j}\right|^2 + \sigma^2}\right) \\ &\qquad + \sum_{i\neq k}^{K}\sum_{m=1}^{L_i}\left|\mathbf{f}_{k,l}\mathbf{H}_k^H\mathbf{w}_{i,m}\right|^2 \end{aligned} \tag{4}$$

A. Problem Formulation

To achieve a predetermined target SE for each user with the minimum transmit power, each user requires an optimal tradeoff between its full diversity obtained with a single stream, i.e., $L_k = 1$, and full multiplexing gains corresponding to $L_k = \min(N_t, N_{r,k})$. This implies that the number of data streams for each user, which provides the optimal tradeoff between diversity and multiplexing gains, will lie between 1 and $\min(N_t, N_{r,k})$, i.e., $1 \leq L_k \leq \min(N_t, N_{r,k})$. Consequently, we aim to determine the number of data streams for all users, i.e., $L_k, \forall k$, which can ensure a target SE performance for all users, i.e., $\lambda_k, \forall k$, in the minimum possible transmit power at the AP. For this purpose we need to optimize the transmit filter $\mathbf{W}$, receive filters $\mathbf{F}_k, \forall k$, number of data streams $L_k, \forall k$, power allocations $p_k, \forall k$, transmit/receive vertical/horizontal phase shifters at DP antennas $\mathbf{U}_p, \mathbf{E}_p^k, p \in \{v, h\}, \forall k$, and DP-IRS operations $\mathbf{\Phi}^{pq}$, where $p, q \in \{v, h\}$. Hence, the problem can be formulated as

$$\begin{aligned} \min_{\mathbf{W},\mathbf{F},L_k,\mathbf{U}^p,\mathbf{\Phi}^{pq},\mathbf{E}_k^p} \ & \sum_{k=1}^{K} p_k \\ \text{s.t.} \quad & f\left(\mathbf{W}, \mathbf{F}, L_k, \mathbf{U}^p, \mathbf{\Phi}^{pq}, \mathbf{E}_k^p\right) \geq \lambda_k, \ \forall k, \\ & \mathbf{\Phi}^{pq} = \text{diag}\left(e^{-j\phi_{pq,1}}, \ldots, e^{-j\phi_{pq,N}}\right), \ p, q \in \{v, h\}, \\ & \mathbf{U}^p = \text{diag}\left(e^{-j\gamma_{p,1}}, \ldots, e^{-j\gamma_{p,N_t}}\right), \ p \in \{v, h\}, \\ & \mathbf{E}_k^p = \text{diag}\left(e^{-j\delta_{p,1}}, \ldots, e^{-j\delta_{p,N_{r,k}}}\right), \ p \in \{v, h\}, \ \forall k, \\ & \sum_{k=1}^{K} p_k \leq P_{\max}, \end{aligned} \tag{P1}$$

where, as mentioned earlier, λ_k represents the minimum SE requirement for the user k, $P_{\max}$ denotes the maximum transmit power available at the AP, and p_k denotes the transmit power allocated to user k. Problem (P1) represents a complex non-convex problem with multiple coupled optimization variables of different natures. Specifically, the first constraint involves a non-concave function with non-convex complex expressions in both the numerator and the denominator. Additionally, the fractions in (P1) exhibit a unique non-convex nature because the discrete variable L_k in the summation for user k is also an optimization variable. This complex optimization framework is unique to the proposed generalized system model in Figure 1 and does not have a standard algorithm in the literature. In the preceding sections, we develop solutions for (P1) and propose two novel multi-step AO algorithms to solve this problem efficiently.

III. Proposed Solution to Problem (P1)

We decompose (P1) into several subproblems, deriving their low-complexity convex formulations. Ultimately, we present a multistep AO algorithm designed to systematically address these subproblems, ensuring the convergence of the Specifically, our contributions to solve (P1) are as follows: 1) We study a novel problem to optimize L_k, as detailed in Section III-A. 2) To address the non-homogeneous quadratic expressions coupled with polarization conversion and splitting, we identify the essential components of the semidefinite formulation. 3) By utilizing fractional programming, we derive a novel convex formulation for per-user multistream optimization. 4) To alleviate the complexity of log-sum expressions, we propose a low-complexity formulation based on the geometric mean.

A. Optimal Transmit/Receive Digital Filters, Number of Data Streams, and Power Allocations

Here, we reformulate (P1) to determine the transmit digital filter at the AP, receive digital filters for the receivers, optimal power allocations p_k, $\forall k$, and number of data streams L_k, $\forall k$. For the purpose, assume $\mathbf{\Phi}^{pq} = \mathbf{I}_{\mathbf{\Phi}^{pq}}$, $\mathbf{U}^p = \mathbf{I}_{\mathbf{U}^p}$, and $\mathbf{E}_k^p = \mathbf{I}_{\mathbf{E}_k^p}$, $\forall k$, where $p, q \in \{v, h\}$. Accordingly, (P1) is reformulated as

$$\begin{aligned} \min_{\mathbf{W},\mathbf{F},L_k,p_k} \ & \sum_{k=1}^{K} p_k \\ \text{s.t.} \quad & \sum_{l=1}^{L_k}\log_2\left(1 + \frac{\left|\mathbf{f}_{k,l}\mathbf{H}_k^H\mathbf{w}_{k,l}\right|^2}{\sum\limits_{j\neq l}^{L_k}\left|\mathbf{f}_{k,l}\mathbf{H}_k^H\mathbf{w}_{k,j}\right|^2 + \sum\limits_{i\neq k}^{K}\sum\limits_{m=1}^{L_i}\left|\mathbf{f}_{k,l}\mathbf{H}_k^H\mathbf{w}_{i,m}\right|^2 + \sigma^2}\right) \\ & \geq \lambda_k, \forall k \\ & \sum_{k=1}^{K}\sum_{l=1}^{L_k}\left\|\mathbf{w}_{k,l}\right\|^2 \leq P_{\max}, \end{aligned} \tag{P1.1}$$

where $\left\|\mathbf{w}_{k,l}\right\|^2$ denotes the power allocated to lth data stream of user k, i.e., $\rho_{k,l} = \left\|\mathbf{w}_{k,l}\right\|^2$ such that $\rho_k = \sum\limits_{l=1}^{L_k}\rho_{k,l}$. To address (P1.1), we introduce a four-step AO algorithm.

Given an initial setup where each user k is assigned a number of data streams L_k and power allocations p_k equal

to $\min(N_t, N_{r,k})$ and $\frac{P_{\max}}{L_k}$ respectively, the matrices $\overline{\mathbf{W}}$ and $\mathbf{F}_k$, i.e., transmit and receive digital filters, for all users are calculated using mutually dependent optimal linear MMSE filters:

$$\overline{\mathbf{W}} = \left[\overline{\mathbf{w}}_{1,1}, \overline{\mathbf{w}}_{1,2}, \cdots, \overline{\mathbf{w}}_{K,\min(N_t,N_{r,K})}\right] \tag{5}$$

and

$$\mathbf{F}_k^H = \left[\mathbf{f}_{k,1}, \mathbf{f}_{k,2}, \cdots, \mathbf{f}_{k,\min(N_t,N_{r,k})}\right], \ \forall k, \tag{6}$$

where $\overline{\mathbf{w}}_{k,l} = \frac{\hat{e}_{\max}\left(\mathbf{S}_{k,l}^{\mathbf{f}_{k,l}}, \mathbf{T}_{k,l}^{\mathbf{f}_{k,l}}\right)}{\left\|\hat{e}_{\max}\left(\mathbf{S}_{k,l}^{\mathbf{f}_{k,l}}, \mathbf{T}_{k,l}^{\mathbf{f}_{k,l}}\right)\right\|}$, $\mathbf{f}_{k,l} = \frac{\hat{e}_{\max}\left(\mathbf{S}_{k,l}^{\overline{\mathbf{w}}_{k,l}}, \mathbf{T}_{k,l}^{\overline{\mathbf{w}}_{k,l}}\right)}{\left\|\hat{e}_{\max}\left(\mathbf{S}_{k,l}^{\overline{\mathbf{w}}_{k,l}}, \mathbf{T}_{k,l}^{\overline{\mathbf{w}}_{k,l}}\right)\right\|}$, $\mathbf{S}_{k,l}^{\mathbf{f}_{k,l}} = \mathbf{H}_k \mathbf{f}_{k,l} \mathbf{f}_{k,l}^H \mathbf{H}_k^H$, $\mathbf{S}_{k,l}^{\overline{\mathbf{w}}_{k,l}} = \mathbf{H}_k^H \overline{\mathbf{w}}_{k,l} \overline{\mathbf{w}}_{k,l}^H \mathbf{H}_k$, $\mathbf{T}_{k,l}^{\mathbf{f}_{k,l}} = \sum_{i \neq k}^{K} \sum_{m=1}^{L_i} \rho_{i,m} \mathbf{H}_i \mathbf{f}_{i,m} \mathbf{f}_{i,m}^H \mathbf{H}_i^H + \sum_{j \neq l}^{L_k} \rho_{k,j} \mathbf{H}_k \mathbf{f}_{k.j} \mathbf{f}_{k.j}^H \mathbf{H}_k^H + \sigma^2 \mathbf{I}$, $\mathbf{T}_{k,l}^{\overline{\mathbf{w}}_{k,l}} = \sum_{i \neq k}^{K} \sum_{m=1}^{L_i} \rho_{i,m} \mathbf{H}_k^H \overline{\mathbf{w}}_{i.m} \overline{\mathbf{w}}_{i.m}^H \mathbf{H}_k + \sum_{j \neq l}^{L_k} \rho_{k,j} \mathbf{H}_k^H \overline{\mathbf{w}}_{k.j} \overline{\mathbf{w}}_{k.j}^H \mathbf{H}_k + \sigma^2 \mathbf{I}$, and $\overline{\mathbf{w}}_{k,l} = \frac{\mathbf{w}_{k,l}}{\|\mathbf{w}_{k,l}\|}$, $\forall l, k$.

Given $\overline{\mathbf{W}}$ and $\mathbf{F}_k, \forall k$ from (5) and (6), respectively, the problem (P1.1) for L_k, $\forall k$, and corresponding p_k, $\forall k$, can be written as

$$\begin{aligned}
\min_{L_k, p_k} \quad & \sum_{k=1}^{K} p_k \\
\text{s.t.} \quad & \sum_{l=1}^{\min(N_t,N_{r,k})} \log_2\left(1 + \tfrac{p_{k,l} e_{k,l}}{r_{k,l} + q_{k,l} + \sigma^2}\right) \geq \lambda_k, \quad \forall k \\
& e_{k,l} = \left|\mathbf{f}_{k,l}^H \mathbf{H}_k^H \bar{\mathbf{w}}_{k,l}\right|^2, \\
& r_{k,l} = \sum_{j \neq l}^{\min(N_t,N_{r,k})} \left|\mathbf{f}_{k,l}^H \mathbf{H}_k^H \sqrt{p_{k.j}} \bar{\mathbf{w}}_{k,j}\right|^2, \\
& q_{k,l} = \sum_{i \neq k}^{K} \sum_{j=1}^{\min(N_t,N_{r,j})} \left|\mathbf{f}_{k,l}^H \mathbf{H}_i^H \sqrt{p_{i,j}} \bar{\mathbf{w}}_{i,j}\right|^2, \\
& \sum_{k=1}^{K} \sum_{l=1}^{\min(N_t,N_{r,k})} p_{k,l} \leq P_{\max}.
\end{aligned} \tag{P1.2}$$

To solve (P1.3), we need to handle the fractions that are coupled with log-sum expressions. We could use traditional fractional programming techniques to deal with the fractions in (P1.3); however, note that L_k is also an optimization variable in addition to p_k. Therefore, before we address the fractions, we first need to handle the log-sum function and maintain its relation with λ_k for all k. To address the log-sum expressions, we define $\min(N_t, N_{r,k})$ optimization variables, denoted as $\lambda_{k,l}$ for all k and l, and replace λ_k with $\sum_{l=1}^{L_k} \lambda_{k,l}$ for all k. Thus, we have:

$$\begin{aligned}
\min_{L_k, p_{k,l}, \lambda_{k,l}} \quad & \sum_{k=1}^{K} \sum_{l=1}^{\min(N_t,N_{r,k})} p_{k,l} \\
\text{s.t.} \quad & \sum_{l=1}^{\min(N_t,N_{r,k})} \log_2\left(1 + \tfrac{p_{k,l} e_{k,l}}{r_{k,l} + q_{k,l} + \sigma^2}\right) \\
& \geq \sum_{l=1}^{\min(N_t,N_{r,k})} \lambda_{k,l} = \lambda_k, \quad \forall k, \\
& \sum_{k=1}^{K} \sum_{l=1}^{\min(N_t,N_{r,k})} p_{k,l} \leq P_{\max}.
\end{aligned} \tag{P1.3}$$

Introducing $\sum_{l=1}^{L_k} \lambda_{k,l} = \lambda_k, \forall k$, as a constraint, (P1.3) can be modified as

$$\begin{aligned}
\min_{L_k, p_{k,l}, \lambda_{k,l}} \quad & \sum_{k=1}^{K} \sum_{l=1}^{\min(N_t,N_{r,k})} p_{k,l} \\
\text{s.t.} \quad & \log_2\left(1 + \tfrac{p_{k,l} e_{k,l}}{r_{k,l} + q_{k,l} + \sigma^2}\right) \geq \lambda_{k,l}, \quad \forall k, l, \\
& \sum_{l=1}^{\min(N_t,N_{r,k})} \lambda_{k,l} = \lambda_k, \quad \forall k, \\
& \sum_{k=1}^{K} \sum_{l=1}^{\min(N_t,N_{r,k})} p_{k,l} \leq P_{\max}.
\end{aligned} \tag{P1.4}$$

Now we have one-to-one correspondence between the left-hand side and right-hand side expressions in the first constraint of (P1.4); Therefore, the convex formulation of (P1.4) can be derived as follows:

$$\begin{aligned}
\min_{L_k, p_{k,l}, \lambda_{k,l}} \quad & \sum_{k=1}^{K} \sum_{l=1}^{\min(N_t,N_{r,k})} p_{k,l} \\
\text{s.t.} \quad & p_{k,l} e_{k,l} - \left(2^{\lambda_{k,l}} - 1\right)\left(r_{k,l} + q_{k,l} + \sigma^2\right) \geq 0, \\
& \forall k, l, \\
& \sum_{l=1}^{\min(N_t,N_{r,k})} \lambda_{k,l} = \lambda_k, \quad \forall k, \\
& \sum_{k=1}^{K} \sum_{l=1}^{\min(N_t,N_{r,k})} p_{k,l} \leq P_{\max}.
\end{aligned} \tag{P1.5}$$

Given $\lambda_{k,l}$ and $p_{k,l}$, $\forall k, l$, from (P1.5), the optimal L_k and p_k, $\forall k$, can be calculated as $\left[p_{k,1,\cdots,}p_{k,\min(N_t,N_{r,k})}\right] > 0$ and $\sum_{l=1}^{\min(N_t,N_{r,k})} \rho_{k,l}$, $\forall k$, respectively. While (P1.5) is convex, we can further simplify it to reduce complexity. Specifically, with $\rho_{k,l} = \frac{P_{\max}}{\sum_{k=1}^{K} \min(N_t,N_{r,k})}$, (P1.5) provides per-iteration optimal values for $\lambda_{k,l}$ across all values of k and l. With these determined $\lambda_{k,l}$, along with $\mathbf{W}$ and $\mathbf{F}_k$, the optimal power allocations can be easily computed as follows:

$$\mathbf{p} = \left(\mathbf{J}^{-1} - \boldsymbol{\omega}\right) \mathbf{1}_{K'}, \tag{7}$$

where $K' = K + \sum_{l=1}^{\min(N_t,N_{r,k})} 1$, $\mathbf{p} = [\rho_{1,1}, \rho_{1,2}, \cdots, \rho_{1,L_1}, \cdots, \rho_{K,\min(N_t,N_{r,k})}]$, $\mathbf{J} =$

$$\text{diag}\left(\frac{\sigma^2\left(2^{\lambda_{1,1}}-1\right)}{\left|\mathbf{f}_{1,1}^H\mathbf{H}_1^H\overline{\mathbf{w}}_{1,1}\right|^2},\frac{\sigma^2\left(2^{\lambda_{1,2}}-1\right)}{\left|\mathbf{f}_{1,2}^H\mathbf{H}_2^H\overline{\mathbf{w}}_{1,2}\right|^2},\cdots,\frac{\sigma^2\left(2^{\lambda_{K,L_K}}-1\right)}{\left|\mathbf{f}_{K,L_K}^H\mathbf{H}_K^H\overline{\mathbf{w}}_{K,L_K}\right|^2}\right)$$

and $\boldsymbol{\omega}_{(r,c)} = \begin{cases} \sigma^2\left|\mathbf{f}_{k,r}^H\mathbf{H}_k^H\overline{\mathbf{w}}_{k,c}\right|^2, & r\neq c \\ 0, & r=c \end{cases}, \forall k.$

A more refined explanation of the optimization process for $\mathbf{W}$, $\mathbf{F}_k$, L_k, and p_k is presented through a systematic four-step AO algorithm, as outlined in Algorithm 1. When provided with the initial values for $\mathbf{W}$, $\mathbf{F}_k$, L_k, and p_k obtained from (5), (6), (P1.5), and (7), the problem (P1) can be expressed as:

$$\begin{aligned}&\max_{\boldsymbol{\Phi}^{pq},\mathbf{U}^p,\mathbf{E}_k^p} f\left(\boldsymbol{\Phi}^{pq},\mathbf{U}^p,\mathbf{E}_k^p\right)\\ &\text{s.t.}\quad c_k\geq\lambda_k,\forall k\\ &\boldsymbol{\Phi}^{pq}=\text{diag}(e^{-j\phi_{pq,1}},\cdots,e^{-j\phi_{pq,N}}),\ p,q\in\{v,h\},\\ &\mathbf{U}^p=\text{diag}(e^{-j\gamma_{p,1}},\cdots,e^{-j\gamma_{p,N_t}}),\ p\in\{v,h\},\\ &\mathbf{E}_k^p=\text{diag}(e^{-j\delta_{p,1}},\cdots,e^{-j\delta_{p,N_{r,k}}}),\ p\in\{v,h\},\ \forall k,\end{aligned} \tag{P1.6}$$

where $f\left(\boldsymbol{\Phi}^{pq},\mathbf{U}^p,\mathbf{E}_k^p\right)$ is defined by (4) when $\mathbf{W}$, $\mathbf{F}_k$, and L_k, for all k, are constant. In the following three subsections, we tackle (P1.6) by developing solutions for $\boldsymbol{\Phi}^{pq}$, $\mathbf{U}^p$, and $\mathbf{E}_k^p$, $\forall k$.

B. Optimization of DP-IRS Phases

Assuming $\mathbf{U}^p=\mathbf{I}_{\mathbf{U}}^p$ and $\mathbf{E}_k^p=\mathbf{I}_{\mathbf{E}_k^p},\forall k$, and by changing variables, we have

$\mathbf{f}_{k,l}^H\mathbf{E}_k^p\left(\mathbf{H}_{r,k}^p\right)^H\boldsymbol{\Phi}^{pq}\mathbf{G}^q\mathbf{U}^p\mathbf{w}_{i,m} = \mathbf{l}_{pq}^H\boldsymbol{\omega}_{qp}^{kl,im}$,
$\mathbf{f}_{k,l}^H\mathbf{E}_k^p\left(\mathbf{H}_{r,k}^p\right)^H\boldsymbol{\Phi}^{pq}\mathbf{G}^q\mathbf{U}^p\mathbf{w}_{k,j} = \mathbf{l}_{pq}^H\boldsymbol{\omega}_{qp}^{kl,kj}$,
$\mathbf{f}_{k,l}^H\mathbf{E}_k^p\left(\mathbf{H}_{d,k}^p\right)^H\mathbf{U}^p\mathbf{w}_{i,m} = \xi_p^{kl,im}$,
$\mathbf{f}_{k,l}^H\mathbf{E}_k^p\left(\mathbf{H}_{d,k}^p\right)^H\mathbf{U}^p\mathbf{w}_{k,j} = \xi_p^{kl,kj}$, where
$\boldsymbol{\omega}_{pq}^{kl,im} = \text{diag}(\mathbf{f}_k^H\mathbf{E}_k^p\left(\mathbf{H}_{r,k}^p\right)^H)\mathbf{G}^q\mathbf{U}^p\mathbf{w}_{i,m}$,
$\boldsymbol{\omega}_{pq}^{kl,kj} = \text{diag}(\mathbf{f}_k^H\mathbf{E}_k^p\left(\mathbf{H}_{r,k}^p\right)^H)\mathbf{G}^q\mathbf{U}^p\mathbf{w}_{k,j}$, and
$\mathbf{l}_{pq}^H = \left[e^{-j\phi_{pq,1}},e^{-j\phi_{pq,2}},\ldots,e^{-j\phi_{pq,N}}\right]$. Thus, (P1.6) is rewritten as

$$\begin{aligned}&\max_{\mathbf{l}_{pp},\mathbf{l}_{pq}}\quad\sum_{k=1}^{K}\sum_{l=1}^{L_k}\log_2\left(1+\frac{e_{kl}}{q_{kl}+r_{kl}+\sigma^2}\right)\\ &\text{s.t.}\\ &e_{kl,pq}=|\mathbf{l}_{vv}^H\boldsymbol{\omega}_{vv}^{kl,kl}+\mathbf{l}_{hv}^H\boldsymbol{\omega}_{vh}^{kl,kl}+\xi_v^{kl,kl}+\mathbf{l}_{hh}^H\boldsymbol{\omega}_{hh}^{kl,kl}\\ &\quad+\mathbf{l}_{vh}^H\boldsymbol{\omega}_{hv}^{kl,kl}+\xi_h^{kl,kl}|^2,\\ &q_{kl,pq}=\sum_{i\neq k}^{K}\sum_{m=1}^{L_i}|\mathbf{l}_{vv}^H\boldsymbol{\omega}_{vv}^{kl,im}+\mathbf{l}_{hv}^H\boldsymbol{\omega}_{vh}^{kl,im}+\xi_v^{kl,im}\\ &\quad+\mathbf{l}_{hh}^H\boldsymbol{\omega}_{hh}^{kl,im}+\mathbf{l}_{vh}^H\boldsymbol{\omega}_{hv}^{kl,im}+\xi_h^{kl,im}|^2,\\ &r_{kl,pq}=\sum_{j\neq l}^{L_k}|\mathbf{l}_{vv}^H\boldsymbol{\omega}_{vv}^{kl,kj}+\mathbf{l}_{hv}^H\boldsymbol{\omega}_{vh}^{kl,kj}+\xi_v^{kl,kj}\\ &\quad+\mathbf{l}_{hh}^H\boldsymbol{\omega}_{hh}^{kl,kj}+\mathbf{l}_{vh}^H\boldsymbol{\omega}_{hv}^{kl,kj}+\xi_h^{kl,kj}|^2,\\ &c_k\geq\lambda_k,\ \forall k,\\ &|\mathbf{l}_{pq_{(n)}}^H|=1,\ n=1,\ldots,N,\ p,q\in\{v,h\},\end{aligned} \tag{P1.8}$$

where the intended signal strength $e_{kl,pq}$, interuser interference $q_{kl,pq}$, and intrauser interference $r_{kl,pq}$ are tunable with respect to $\mathbf{l}_{pp}$ and $\mathbf{l}_{pq}$ for all k,l, and are addressed in the following subsections.

1) Optimization of Vertical to Vertical Phase Shifts: Defining

$$\xi_{vv}^{kl,im}=\mathbf{l}_{hv}^H\boldsymbol{\omega}_{vh}^{kl,im}+\xi_v^{kl,im}+\mathbf{l}_{hh}^H\boldsymbol{\omega}_{hh}^{kl,im}+\mathbf{l}_{vh}^H\boldsymbol{\omega}_{hv}^{kl,im}+\xi_h^{kl,im}$$

and

$$\xi_{vv}^{kl,kj}=\mathbf{l}_{hv}^H\boldsymbol{\omega}_{vh}^{kl,kj}+\xi_v^{kl,kj}+\mathbf{l}_{hh}^H\boldsymbol{\omega}_{hh}^{kl,kj}+\mathbf{l}_{vh}^H\boldsymbol{\omega}_{hv}^{kl,kj}+\xi_h^{kl,kj},$$

where $\mathbf{l}_{hv}^H=\mathbf{l}_{hh}^H=\mathbf{l}_{vh}^H=[1,1,1,\cdots,1]$, (P1.8) for $\mathbf{l}_{vv}$ can be written as (P1.9). Inserting

$$\begin{aligned}|\mathbf{l}_{vv}^H\boldsymbol{\omega}_{vv}^{kl,im}+\xi_{vv}^{kl,im}|^2=&\,\mathbf{l}_{vv}^H\boldsymbol{\omega}_{vv}^{kl,im}\boldsymbol{\omega}_{vv}^{kl,im^H}\mathbf{l}_{vv}\\&+\mathbf{l}_{vv}^H\boldsymbol{\omega}_{vv}^{kl,im}\xi_{vv}^{kl,im^H}+\xi_{vv}^{kl,im}\boldsymbol{\omega}_{vv}^{kl,im^H}\mathbf{l}_{vv}+|\xi_{vv}^{kl,im}|^2\end{aligned}$$

and

$$\begin{aligned}|\mathbf{l}_{vv}^H\boldsymbol{\omega}_{vv}^{kl,jk}+\xi_{vv}^{kl,jk}|^2=&\,\mathbf{l}_{vv}^H\boldsymbol{\omega}_{vv}^{kl,jk}\boldsymbol{\omega}_{vv}^{kl,jk^H}\mathbf{l}_{vv}\\&+\mathbf{l}_{vv}^H\boldsymbol{\omega}_{vv}^{kl,jk}\xi_{vv}^{kl,jk^H}+\xi_{vv}^{kl,jk}\boldsymbol{\omega}_{vv}^{kl,jk^H}\mathbf{l}_{vv}+|\xi_{vv}^{kl,jk}|^2\end{aligned}$$

we have (P1.10).

$$\begin{aligned}\max_{\mathbf{l}_{vv}}\quad&\sum_{k=1}^{K}\sum_{l=1}^{L_k}\log_2\left(1+\frac{\left|\mathbf{l}_{vv}^H\boldsymbol{\omega}_{vv}^{kl,kl}+\xi_{vv}^{kl,kl}\right|^2}{\sum_{i\neq k}^{K}\sum_{m=1}^{L_i}\left|\mathbf{l}_{vv}^H\boldsymbol{\omega}_{vv}^{kl,im}+\xi_{vv}^{kl,im}\right|^2+\sum_{j\neq l}^{L_k}\left|\mathbf{l}_{vv}^H\boldsymbol{\omega}_{vv}^{kl,kj}+\xi_{vv}^{kl,kj}\right|^2+\sigma^2}\right)\\&\text{s.t.}\quad c_k\geq\lambda_k,\ \forall k,\\&\quad\left|\mathbf{l}_{vv_{(n)}}^H\right|=1,\ n=1,\ldots,N.\end{aligned} \tag{P1.9}$$

$$\begin{aligned}\max_{\mathbf{l}_{vv}}\quad&\sum_{k=1}^{K}\sum_{l=1}^{L_k}\log_2\left(1+\frac{e_{kl,vv}}{r_{kl,vv}+q_{kl,vv}+\sigma^2}\right)\\&\text{s.t.}\\&e_{kl,vv}=\mathbf{l}_{vv}^H\boldsymbol{\omega}_{vv}^{kl,kl}\boldsymbol{\omega}_{vv}^{kl,l^H}\mathbf{l}_{vv}+\mathbf{l}_{vv}^H\boldsymbol{\omega}_{vv}^{kl,kl}\xi_{vv}^{kl,l^H}\\&\quad+\left|\xi_{vv}^{kl,kl}\right|^2+\xi_{vv}^{kl,kl}\boldsymbol{\omega}_{vv}^{kl,l^H}\mathbf{l}_{vv},\\&r_{kl,vv}=\sum_{i\neq k}^{K}\sum_{m=1}^{L_i}\mathbf{l}_{vv}^H\boldsymbol{\omega}_{vv}^{kl,im}\boldsymbol{\omega}_{vv}^{kl,m^H}\mathbf{l}_{vv}+\xi_{vv}^{kl,im}\boldsymbol{\omega}_{vv}^{kl,m^H}\mathbf{l}_{vv}\\&\quad+\mathbf{l}_{vv}^H\boldsymbol{\omega}_{vv}^{kl,im}\xi_{vv}^{kl,m^H}+\left|\xi_{vv}^{kl,im}\right|^2,\\&q_{kl,vv}=\sum_{j\neq l}^{L_k}\mathbf{l}_{vv}^H\boldsymbol{\omega}_{vv}^{kl,jk}\boldsymbol{\omega}_{vv}^{kl,k^H}\mathbf{l}_{vv}\\&\quad+\mathbf{l}_{vv}^H\boldsymbol{\omega}_{vv}^{kl,jk}\xi_{vv}^{kl,k^H}+\left|\xi_{vv}^{kl,jk}\right|^2+\xi_{vv}^{kl,jk}\boldsymbol{\omega}_{vv}^{kl,k^H}\mathbf{l}_{vv},\\&c_k\geq\lambda_k,\ \forall k,\quad\left|\mathbf{l}_{vv_{(n)}}^H\right|=1,\ n=1,\ldots,N.\end{aligned} \tag{P1.10}$$

Defining

$$\boldsymbol{\Theta}_{vv}^{kl,kl}=\begin{bmatrix}\boldsymbol{\omega}_{vv}^{kl,kl}\boldsymbol{\omega}_{vv}^{kl,kl^H} & \boldsymbol{\omega}_{vv}^{kl,kl}\xi_{vv}^{kl,kl^H}\\ \boldsymbol{\omega}_{vv}^{kl,kl^H}\xi_{vv}^{kl,kl} & 0\end{bmatrix},$$

$$\boldsymbol{\Theta}_{vv}^{kl,im}=\begin{bmatrix}\boldsymbol{\omega}_{vv}^{kl,im}\boldsymbol{\omega}_{vv}^{kl,im^H} & \boldsymbol{\omega}_{vv}^{kl,im}\xi_{vv}^{kl,im^H}\\ \boldsymbol{\omega}_{vv}^{kl,im^H}\xi_{vv}^{kl,im} & 0\end{bmatrix},$$

and $\bar{\mathbf{l}}_{vv} = \begin{bmatrix} \mathbf{l}_{vv} \\ t_{vv} \end{bmatrix}$, where t_{vv} is an auxiliary variable, the numerator and denominator expressions in (P1.10) can be homogenized as

$$\max_{\mathbf{l}_{vv}} \sum_{k=1}^{K}\sum_{l=1}^{L_k} \log_2\left(1 + \frac{\bar{\mathbf{l}}_{vv}^H \boldsymbol{\Theta}_{vv}^{kl,kl} \bar{\mathbf{l}}_{vv} + \left|\xi_{vv}^{kl,kl}\right|^2}{\sum\limits_{i\neq k}^{K}\sum\limits_{m=1}^{L_i}\left(\bar{\mathbf{l}}_{vv}^H \boldsymbol{\Theta}_{vv}^{kl,im} \bar{\mathbf{l}}_{vv} + \left|\xi_{vv}^{kl,im}\right|^2\right) + \sum\limits_{j\neq l}^{L_k}\left(\bar{\mathbf{l}}_{vv}^H \boldsymbol{\Theta}_{vv}^{kl,kj} \bar{\mathbf{l}}_{vv} + \left|\xi_{vv}^{kl,kj}\right|^2\right) + \sigma^2}\right)$$

s.t.

$$\begin{aligned} &c_k \geq \lambda_k,\ \forall k, \\ &\left|\bar{\mathbf{l}}_{vv_{(n)}}^H\right| = 1,\ n = 1, \ldots, N+1. \end{aligned} \tag{P1.11}$$

Defining $\bar{\mathbf{l}}_{vv}^H \boldsymbol{\Theta}_{vv} \bar{\mathbf{l}}_{vv} = \mathrm{trace}\left(\boldsymbol{\Theta}_{vv} \bar{\mathbf{l}}_{vv} \bar{\mathbf{l}}_{vv}^H\right) = \mathrm{trace}\left(\boldsymbol{\Theta}_{vv} \mathbf{L}_{vv}\right)$, where $\mathbf{L}_{vv} = \bar{\mathbf{l}}_{vv} \bar{\mathbf{l}}_{vv}^H$ must be rank 1, i.e., $\mathrm{rank}\left(\mathbf{L}_{vv}\right) = 1$, we have semidefinite expressions

$$\max_{\mathbf{L}_{vv}} \sum_{k=1}^{K}\sum_{l=1}^{L_k} \log_2\left(1 + \frac{\mathrm{trace}\left(\boldsymbol{\Theta}_{vv}^{kl,kl} \mathbf{L}_{vv}\right) + \left|\xi_{vv}^{kl,kl}\right|^2}{\sum_{i\neq k}^{K}\sum_{m=1}^{L_i}\mathrm{trace}\left(\boldsymbol{\Theta}_{vv}^{kl,im} \mathbf{L}_{vv}\right) + \sum_{j\neq l}^{L_k}\mathrm{trace}\left(\boldsymbol{\Theta}_{vv}^{kl,jk} \mathbf{L}_{vv}\right) + \sigma^2 + \sum_{i\neq k}^{K}\sum_{m=1}^{L_i}\left|\xi_{vv}^{kl,im}\right|^2}\right)$$

s.t.

$$\begin{aligned} &c_k \geq \lambda_k,\ \forall k, \quad \mathrm{rank}\left(\mathbf{L}_{vv}\right) = 1, \quad \mathbf{L}_{vv} \succ 0, \\ &\mathbf{L}_{vv_{(n,n)}} = 1,\ n = 1, \ldots, N+1. \end{aligned} \tag{P1.12}$$

By relaxing the rank-1 constraint, both the numerator and denominator expressions become convex. However, the presence of fractions retains a nonconvex nature, leading to a nonconcave problem. Utilizing fractional programming techniques [29], we derive the convex formulation of (P1.12) as follows:

$$\begin{aligned} \max_{\mathbf{L}_{vv},\{y_{kl}\}} & \sum_{k=1}^{K}\sum_{l=1}^{L_k} \log_2\Bigg(1 + 2y_{kl}\left(\mathrm{trace}\left(\boldsymbol{\Theta}_{vv}^{kl,kl}\mathbf{L}_{vv}\right) + \left|\xi_{vv}^{kl,kl}\right|^2\right) \\ & - y_{kl}^2\left[\sum_{i\neq k}^{K}\sum_{m=1}^{L_i}\left(\mathrm{trace}\left(\boldsymbol{\Theta}_{vv}^{kl,im}\mathbf{L}_{vv}\right) + \left|\xi_{vv}^{kl,im}\right|^2\right) \right. \\ & \left. + \sum_{j\neq l}^{L_k}\left(\mathrm{trace}\left(\boldsymbol{\Theta}_{vv}^{kl,jk}\mathbf{L}_{vv}\right) + \left|\xi_{vv}^{kl,jk}\right|^2\right) + \sigma^2\right]\Bigg) \end{aligned}$$

s.t.

$$\begin{aligned} &y_{kl} \in \mathbb{R},\ \forall k, l, \quad c_k \geq \lambda_k,\ \forall k, \quad \mathbf{L}_{vv} \succ 0, \\ &\mathbf{L}_{vv_{(n,n)}} = 1,\ n = 1, \ldots, N+1, \end{aligned} \tag{P1.13}$$

where $y_{kl},\ \forall k, l$, represents extra optimization variables that serve as weights requiring optimization for optimal results. Despite its simplified and convex nature, (P1.13) still a complex problem primarily due to the following reasons:

1) Log-sum expressions are computationally expensive to solve (the reader is referred to [30] for more details).
2) As part of the multistep AO algorithm, solving (P1.13) does not guarantee convergence.

To address the first issue, we propose replacing the logsum function with the geometric mean (GM), as demonstrated in [30], [31]. Defining $\mathbf{x}_{\mathbf{L}_{vv}}^k = \left[x_{\mathbf{L}_{vv}}^{k,1}, \cdots, x_{\mathbf{L}_{vv}}^{k,L_k}\right]$, where

$$\begin{aligned} x_{\mathbf{L}_{vv}}^{k,l} = 1 &+ 2y_{kl}\left(\mathrm{trace}\left(\boldsymbol{\Theta}_{vv}^{kl,kl}\mathbf{L}_{vv}\right) + |\xi_{vv}^{kl,kl}|^2\right) \\ &- y_{kl}^2\sum_{i\neq k}^{K}\sum_{m=1}^{L_i}\left(\mathrm{trace}\left(\boldsymbol{\Theta}_{vv}^{kl,im}\mathbf{L}_{vv}\right) + |\xi_{vv}^{kl,im}|^2\right) \\ &- y_{kl}^2\sum_{i\neq k}^{K}\left(\mathrm{trace}\left(\boldsymbol{\Theta}_{vv}^{kl,kj}\mathbf{L}_{vv}\right) + |\xi_{vv}^{kl,kj}|^2\right) + \sigma^2, \quad \forall k, l \end{aligned}$$

the objective function of (P1.13), i.e.,

$$\begin{aligned} &\sum_{k=1}^{K}\sum_{l=1}^{L_k}\log_2\left(1 + 2y_{kl}\mathrm{trace}\left(\boldsymbol{\Theta}_{vv}^{kl,kl}\mathbf{L}_{vv}\right) + |\xi_{vv}^{kl,kl}|^2\right. \\ &\quad - y_{kl}^2\sum_{i\neq k}^{K}\left(\mathrm{trace}\left(\boldsymbol{\Theta}_{vv}^{kl,kj}\mathbf{L}_{vv}\right) + |\xi_{vv}^{kl,kj}|^2\right) \\ &\quad \left. - y_{kl}^2\sum_{i\neq k}^{K}\sum_{m=1}^{L_i}\left(\mathrm{trace}\left(\boldsymbol{\Theta}_{vv}^{kl,im}\mathbf{L}_{vv}\right) + |\xi_{vv}^{kl,im}|^2\right) + \sigma^2\right) \end{aligned}$$

can be replaced by $\sum\limits_{k=1}^{K}\mathrm{GM}\left(\mathbf{x}_k\right)$ and the problem (P1.13) is updated as:

$$\begin{aligned} \max_{\mathbf{L}_{vv},\{y_{kl}\}} & \sum_{k=1}^{L_k}\mathrm{GM}\left(\mathbf{x}_k\right) \\ \text{s.t.} \quad & \mathrm{GM}\left(\mathbf{x}_k\right) \geq \lambda_k,\ \forall k, \\ & \mathbf{L}_{vv} \succ 0,\ y_{kl} \in \mathbb{R},\ \forall k, l, \\ & \mathbf{L}_{vv_{(n,n)}} = 1,\ n = 1, \ldots, N+1. \end{aligned} \tag{P1.14}$$

To address the second issue, concerning convergence behavior, we update (P1.14) as follows:

$$\begin{aligned} \max_{\mathbf{L}_{vv},\{y_{kl}\}} & \sum_{k=1}^{L_k}\mathrm{GM}\left(\mathbf{x}_k\right) \\ \text{s.t.} \quad & \mathrm{GM}\left(\mathbf{x}_k\right) \geq \zeta_{vv}^k,\ \forall k, \\ & \mathbf{L}_{vv} \succ 0,\ y_{kl} \in \mathbb{R},\ \forall k, l, \\ & \mathbf{L}_{vv_{(n,n)}} = 1,\ n = 1, \ldots, N+1, \end{aligned} \tag{P1.15}$$

where $\zeta_{\mathbf{L}_{vv}}^k, \forall k$, represents a positive real number selected in each AO algorithm iteration, ensuring the objective value does not increase, guaranteeing convergence. Additional details on the selection of $\zeta_{\mathbf{L}_{vv}}^k$ can be found in Section III-E.

For enhanced simplicity, we introduce slack variables and reformulate the problem as follows:

$$\begin{aligned} \max_{\mathbf{L}_{vv},\{y_{kl}\}} & \sum_{k=1}^{K} o_{\mathbf{L}_{vv}}^k \\ \text{s.t.} \quad & \mathrm{GM}\left(\mathbf{x}_k\right) \geq \zeta_{vv}^k + o_{\mathbf{L}_{vv}}^k,\ \forall k, \\ & \mathbf{L}_{vv} \succ 0,\ y_{kl} \in \mathbb{R},\ \forall k, l, \\ & \mathbf{L}_{vv_{(n,n)}} = 1,\ n = 1, \ldots, N+1. \end{aligned} \tag{P1.16}$$

Problem (P1.16) is convex and can be efficiently solved using CVX[1]. Due to the GM expressions, (P1.15) necessitates a lower computational cost compared to (P1.13) with logsum expressions. Further insights into convergence behavior and computational complexity are discussed in Section V.

2) Optimization of Horizontal to Vertical Phase Shifts: Defining $\xi_{hv}^{kl,im} = \mathbf{l}_{vv}^H \boldsymbol{\omega}_{vv}^{kl,im} + \xi_v^{kl,im} + \mathbf{l}_{hh}^H \boldsymbol{\omega}_{hh}^{kl,im} + \mathbf{l}_{vh}^H \boldsymbol{\omega}_{hv}^{kl,im} + \xi_h^{kl,im}$, $\xi_{hv}^{kl,kj} = \mathbf{l}_{vv}^H \boldsymbol{\omega}_{vv}^{kl,kj} + \xi_v^{kl,kj} + \mathbf{l}_{hh}^H \boldsymbol{\omega}_{hh}^{kl,kj} + \mathbf{l}_{vh}^H \boldsymbol{\omega}_{hv}^{kl,kj} + \xi_h^{kl,kj}$, where $\mathbf{I}_{vv}$ is optimized by solving problem (P1.16), the problem (P1.8) for $\mathbf{I}_{hv}$ can be written as

$$\begin{aligned} \max_{\mathbf{l}_{hv}} \sum_{k=1}^{K} \sum_{l=1}^{L_k} \log_2\left(1 + \frac{e_{kl,hv}}{r_{kl,hv} + q_{kl,hv} + \sigma^2}\right) \\ \text{s.t.} \quad c_k \geq \lambda_k, \forall k, \ \left|\mathbf{l}_{vv_{(n)}}^H\right| = 1, \ n = 1, \cdots, N. \end{aligned} \tag{P1.17}$$

Defining $\boldsymbol{\Theta}_{vh}^{kl,im} = \begin{bmatrix} \boldsymbol{\omega}_{vh}^{kl,im} \boldsymbol{\omega}_{vh}^{kl,im^H} & \boldsymbol{\omega}_{vh}^{kl,im} \xi_{hv}^{kl,im^H} \\ \boldsymbol{\omega}_{vh}^{kl,im^H} \xi_{hv}^{kl,im} & 0 \end{bmatrix}$, $\boldsymbol{\Theta}_{vh}^{kl,kj} = \begin{bmatrix} \boldsymbol{\omega}_{vh}^{kl,kj} \boldsymbol{\omega}_{vh}^{kl,kj^H} & \boldsymbol{\omega}_{vh}^{kl,kj} \xi_{hv}^{kl,kj^H} \\ \boldsymbol{\omega}_{vh}^{kl,kj^H} \xi_{hv}^{kl,kj} & 0 \end{bmatrix}$, and $\bar{\mathbf{l}}_{hv} = \begin{bmatrix} \mathbf{l}_{hv} \\ t_{hv} \end{bmatrix}$, the problem (P1.17) can be homogenized as

$$\begin{aligned} \max_{\mathbf{l}_{hv}} \sum_{k=1}^{K} \sum_{l=1}^{L_k} \log_2\left(1 + \frac{\bar{\mathbf{l}}_{hv}^H \boldsymbol{\Theta}_{vh}^{kl,kl} \bar{\mathbf{l}}_{hv} + \left|\xi_{hv}^{kl,kl}\right|^2}{\sum_{i \neq k}^{K} \sum_{m=1}^{L_i} \left(\bar{\mathbf{l}}_{hv}^H \boldsymbol{\Theta}_{vh}^{kl,im} \bar{\mathbf{l}}_{hv} + \left|\xi_{hv}^{kl,im}\right|^2\right) + \sum_{j \neq l}^{L_K} \left(\bar{\mathbf{l}}_{hv}^H \boldsymbol{\Theta}_{vh}^{kl,kj} \bar{\mathbf{l}}_{hv} + \left|\xi_{hv}^{kl,kj}\right|^2\right) + \sigma^2}\right) \\ \text{s.t.} \quad c_k \geq \lambda_k, \forall k, \quad \left|\bar{\mathbf{l}}_{hv_{(n)}}^H\right| = 1, \, n = 1, \cdots, N+1. \end{aligned} \tag{P1.18}$$

Similar to (P1.11) and sharing analogous issues as discussed in the context of (P1.13), the final convex formulation of (P1.18) can be derived by following the same steps employed for (P1.11):

$$\begin{aligned} \max_{\mathbf{L}_{hv}, y_{kl}} \sum_{k=1}^{K} o_{\mathbf{L}_{hv}}^k \\ \text{s.t.} \quad \text{GM}\left(\mathbf{x}_{\mathbf{L}_{hv}}^k\right) \geq \zeta_{hv}^k + o_{\mathbf{L}_{hv}}^k, \forall k, \\ \mathbf{L}_{hv} \succ 0, \quad y_{kl} \in \mathbb{R}, \forall k, l, \\ \mathbf{L}_{hv_{(n,n)}} = 1, \, n = 1, \cdots, N+1. \end{aligned} \tag{P1.19}$$

where $\mathbf{x}_{\mathbf{L}_{hv}}^k = [x_{\mathbf{L}_{hv}}^{k,1}, \cdots, x_{\mathbf{L}_{hv}}^{k,L_k}]$,

$$\begin{aligned} x_{\mathbf{L}_{hv}}^{k,l} = 1 + 2 y_{kl} \left(\text{trace}\left(\boldsymbol{\Theta}_{vh}^{kl,kl} \mathbf{L}_{hv}\right) + \left|\xi_{hv}^{kl,kl}\right|^2\right) \\ - y_{kl}^2 \sum_{i \neq k}^{K} \sum_{m=1}^{L_i} \left(\text{trace}\left(\boldsymbol{\Theta}_{vh}^{kl,im} \mathbf{L}_{hv}\right) + \left|\xi_{hv}^{kl,im}\right|^2\right) \\ - y_{kl}^2 \sum_{i \neq k}^{K} \left(\text{trace}\left(\boldsymbol{\Theta}_{vh}^{kl,kj} \mathbf{L}_{hv}\right) + \left|\xi_{hv}^{kl,kj}\right|^2\right) + \sigma^2, \end{aligned}$$

$\forall k, l, \ \text{trace}\left(\boldsymbol{\Theta}_{vh} \mathbf{L}_{hv}\right) = \bar{\mathbf{l}}_{hv}^H \boldsymbol{\Theta}_{vh} \bar{\mathbf{l}}_{hv}$, $\mathbf{L}_{hv} = \bar{\mathbf{l}}_{hv} \bar{\mathbf{l}}_{hv}^H$, $o_{\mathbf{L}_{hv}}^{k,l}$ is a slack variable and $\zeta_{\mathbf{L}_{hv}}^{k,l}$ is a real positive variable $\forall k, l$.

[1]Retrieving feasible $\boldsymbol{\Phi}^{vv}$ from $\mathbf{L}_{vv}$ may require additional steps, details are provided in [32] and omitted here for brevity.

3) Optimal Vertical to Horizontal and Horizontal to Horizontal Phase Shifts: Defining $\xi_{hh}^{kl,kj} = \mathbf{l}_{hh}^H \boldsymbol{\omega}_{hh}^{kl,kj} + \xi_v^{kl,kj} + \mathbf{l}_{hh}^H \boldsymbol{\omega}_{hh}^{kl,kj} + \mathbf{l}_{hh}^H \boldsymbol{\omega}_{hh}^{kl,kj} + \xi_h^{kl,kj}$, $\xi_{vh}^{kl,kj} = \mathbf{l}_{vh}^H \boldsymbol{\omega}_{hv}^{kl,kj} + \xi_v^{kl,kj} + \mathbf{l}_{vh}^H \boldsymbol{\omega}_{hv}^{kl,kj} + \mathbf{l}_{vh}^H \boldsymbol{\omega}_{hv}^{kl,kj} + \xi_h^{kl,kj}$, where $\mathbf{l}_{hv}$ and $\mathbf{l}_{vv}$ are retrieved from $\mathbf{L}_{hv}$ and $\mathbf{L}_{vv}$ by solving (P1.18) and (P1.15), respectively, the problem for $\mathbf{l}_{vh}$ and $\mathbf{l}_{hh}$ can be written as

$$\begin{aligned} \max_{\mathbf{l}_{hh}} \sum_{k=1}^{K} \sum_{l=1}^{L_k} \log_2\left(1 + \frac{e_{kl,hh}}{r_{kl,hh} + q_{kl,hh} + \sigma^2}\right) \\ \text{s.t.} \quad c_k \geq \lambda_k, \forall k, \ \left|\mathbf{l}_{hh_{(n)}}^H\right| = 1, \ n = 1, \cdots, N. \\ e_{kl,hh} = \mathbf{l}_{hh}^H \boldsymbol{\omega}_{hh}^{kl,kl} \boldsymbol{\omega}_{hh}^{kl,kl^H} \mathbf{l}_{hh} + \mathbf{l}_{hh}^H \boldsymbol{\omega}_{hh}^{kl,kl} \xi_{hh}^{kl,kl^H} + \left|\xi_{hh}^{kl,kl}\right|^2 \\ \quad + \xi_{hh}^{kl,kl} \boldsymbol{\omega}_{hh}^{kl,kl^H} \mathbf{l}_{hh} \\ r_{kl,hh} = \sum_{i \neq k}^{K} \sum_{m=1}^{L_i} \mathbf{l}_{hh}^H \boldsymbol{\omega}_{hh}^{kl,im} \boldsymbol{\omega}_{hh}^{kl,im^H} \mathbf{l}_{hh} + \mathbf{l}_{hh}^H \boldsymbol{\omega}_{hh}^{kl,im} \xi_{hh}^{kl,im^H} \\ \quad + \xi_{hh}^{kl,im} \boldsymbol{\omega}_{hh}^{kl,im^H} \mathbf{l}_{hh} + \left|\xi_{hh}^{kl,im}\right|^2 \\ q_{kl,hh} = \sum_{j \neq l}^{L_K} \mathbf{l}\mathbf{l}_{hh}^H \boldsymbol{\omega}_{hh}^{kl,jk} \boldsymbol{\omega}_{hh}^{kl,jk^H} \mathbf{l}_{hh} + \mathbf{l}_{hh}^H \boldsymbol{\omega}_{hh}^{kl,jk} \xi_{hh}^{kl,jk^H} \\ \quad + \xi_{hh}^{kl,jk} \boldsymbol{\omega}_{hh}^{kl,jk^H} \mathbf{l}_{hh} + \left|\xi_{hh}^{kl,jk}\right|^2, \end{aligned} \tag{P1.20}$$

and

$$\begin{aligned} \max_{\mathbf{l}_{vh}} \sum_{k=1}^{K} \sum_{l=1}^{L_k} \log_2\left(1 + \frac{e_{kl,vh}}{r_{kl,vh} + q_{kl,vh} + \sigma^2}\right) \\ \text{s.t.} \quad c_k \geq \lambda_k, \forall k, \ \left|\mathbf{l}_{vh_{(n)}}^H\right| = 1, \ n = 1, \cdots, N. \\ e_{kl,vh} = \mathbf{l}_{vh}^H \boldsymbol{\omega}_{hv}^{kl,kl} \boldsymbol{\omega}_{vh}^{kl,kl^H} \mathbf{l}_{hv} + \mathbf{l}_{vh}^H \boldsymbol{\omega}_{hv}^{kl,kl} \xi_{vh}^{kl,kl^H} + \left|\xi_{vh}^{kl,kl}\right|^2 \\ \quad + \xi_{vh}^{kl,kl} \boldsymbol{\omega}_{hv}^{kl,kl^H} \mathbf{l}_{vh}, \forall k \\ r_{kl,vh} = \sum_{i \neq k}^{K} \sum_{m=1}^{L_i} \mathbf{l}_{vh}^H \boldsymbol{\omega}_{hv}^{kl,im} \boldsymbol{\omega}_{hv}^{kl,im^H} \mathbf{l}_{vh} + \mathbf{l}_{vh}^H \boldsymbol{\omega}_{hv}^{kl,im} \xi_{vh}^{kl,im^H} \\ \quad + \xi_{vh}^{kl,im} \boldsymbol{\omega}_{hv}^{kl,im^H} \mathbf{l}_{vh} + \left|\xi_{vh}^{kl,im}\right|^2, \forall k \\ q_{kl,vh} = \sum_{j \neq l}^{L_K} \mathbf{l}_{vh}^H \boldsymbol{\omega}_{hv}^{kl,jk} \boldsymbol{\omega}_{hv}^{kl,jk^H} \mathbf{l}_{vh} + \mathbf{l}_{vh}^H \boldsymbol{\omega}_{hv}^{kl,jk} \xi_{vh}^{kl,jk^H} \\ \quad + \xi_{vh}^{kl,jk} \boldsymbol{\omega}_{hv}^{kl,jk^H} \mathbf{l}_{vh} + \left|\xi_{vh}^{kl,jk}\right|^2, \forall k, \end{aligned} \tag{P1.21}$$

respectively. Problems (P1.20) and (P1.21) share similarities with (P1.10) and (P1.17), respectively. Employing analogous approaches used for $\mathbf{l}_{hv}$ and $\mathbf{l}_{vv}$, respectively, results in the derivation of conclusive convex formulations for $\mathbf{l}_{vh}$ and $\mathbf{l}_{hh}$ as follows:

$$\begin{aligned} \max_{\mathbf{L}_{hh}, y_{kl}} \sum_{k=1}^{K} o_{\mathbf{L}_{hh}}^k \\ \text{s.t. GM}\left(\mathbf{x}_{\mathbf{L}_{\mathbf{hh}}}^{\mathbf{k}}\right) \geq \zeta_{hh}^k + o_{\mathbf{L}_{hh}}^k, \forall k, \\ \mathbf{L}_{hh} \succ 0, \, y_{kl} \in \mathbb{R}, \forall k, l, \\ \mathbf{L}_{hh\,(n,n)} = 1, \, n = 1, \cdots, N+1 \end{aligned} \tag{P1.22}$$

and

$$\begin{aligned} \max_{\mathbf{L}_{vh}, y_{kl}} \sum_{k=1}^{K} o_{\mathbf{L}_{vh}}^k \\ \text{s.t. GM}\left(\mathbf{x}_{\mathbf{L}_{\mathbf{vh}}}^{\mathbf{k}}\right) \geq \zeta_{vh}^k + o_{\mathbf{L}_{vh}}^k, \forall k, \\ \mathbf{L}_{vh} \succ 0, \, y_{kl} \in \mathbb{R}, \forall k, l, \\ \mathbf{L}_{vh\,(n,n)} = 1, \, n = 1, \cdots, N+1 \end{aligned} \tag{P1.23}$$

respectively, where $\mathbf{x}^k_{\mathbf{L}_{hh}} = \left[x^{k,1}_{\mathbf{L}_{hh}}, \cdots, x^{k,L_k}_{\mathbf{L}_{hh}}\right]$, $\mathbf{x}^k_{\mathbf{L}_{vh}} = \left[x^{k,1}_{\mathbf{L}_{vh}}, \cdots, x^{k,L_k}_{\mathbf{L}_{vh}}\right]$,

$$\begin{aligned} x^{k,l}_{\mathbf{L}_{hh}} &= 1 + 2y_{kl}\left(\text{trace}\left(\mathbf{\Theta}^{kl,kl}_{hh}\mathbf{L}_{hh}\right) + \left|\xi^{kl,kl}_{hh}\right|^2\right) \\ &\quad - y^2_{kl}\sum_{i\neq k}^{K}\sum_{m=1}^{L_i}\left(\text{trace}\left(\mathbf{\Theta}^{kl,im}_{hh}\mathbf{L}_{hh}\right) + \left|\xi^{kl,im}_{hh}\right|^2\right) \\ &\quad - y^2_{kl}\sum_{i\neq k}^{K}\left(\text{trace}\left(\mathbf{\Theta}^{kl,kj}_{hh}\mathbf{L}_{hh}\right) + \left|\xi^{kl,kj}_{hh}\right|^2\right) + \sigma^2, \end{aligned} \tag{8}$$

$$\begin{aligned} x^{k,l}_{\mathbf{L}_{vh}} &= 1 + 2y_{kl}\left(\text{trace}\left(\mathbf{\Theta}^{kl,kl}_{vh}\mathbf{L}_{vh}\right) + \left|\xi^{kl,kl}_{vh}\right|^2\right) \\ &\quad - y^2_{kl}\sum_{i\neq k}^{K}\sum_{m=1}^{L_i}\left(\text{trace}\left(\mathbf{\Theta}^{kl,im}_{vh}\mathbf{L}_{vh}\right) + \left|\xi^{kl,im}_{vh}\right|^2\right) \\ &\quad - y^2_{kl}\sum_{i\neq k}^{K}\left(\text{trace}\left(\mathbf{\Theta}^{kl,kj}_{vh}\mathbf{L}_{vh}\right) + \left|\xi^{kl,kj}_{vh}\right|^2\right) + \sigma^2, \end{aligned} \tag{9}$$

$$\mathbf{\Theta}^{kl,im}_{hh} = \begin{bmatrix} \boldsymbol{\omega}^{kl,im}_{hh}\boldsymbol{\omega}^{kl,im^H}_{hh} & \boldsymbol{\omega}^{kl,im}_{hh}\xi^{kl,im^H}_{hh} \\ \boldsymbol{\omega}^{kl,im^H}_{hh}\xi^{kl,im}_{hh} & 0 \end{bmatrix},$$

$$\mathbf{\Theta}^{kl,kj}_{hh} = \begin{bmatrix} \boldsymbol{\omega}^{kl,kj}_{hh}\boldsymbol{\omega}^{kl,im^H}_{hh} & \boldsymbol{\omega}^{kl,kj}_{hh}\xi^{kl,kj^H}_{hh} \\ \boldsymbol{\omega}^{kl,kj^H}_{hh}\xi^{kl,kj}_{hh} & 0 \end{bmatrix},$$

$$\mathbf{\Theta}^{kl,im}_{hv} = \begin{bmatrix} \boldsymbol{\omega}^{kl,im}_{hv}\boldsymbol{\omega}^{kl,im^H}_{hv} & \boldsymbol{\omega}^{kl,im}_{hv}\xi^{kl,im^H}_{vh} \\ \boldsymbol{\omega}^{kl,im^H}_{hv}\xi^{kl,im}_{vh} & 0 \end{bmatrix},$$

$$\mathbf{\Theta}^{kl,kj}_{hv} = \begin{bmatrix} \boldsymbol{\omega}^{kl,kj}_{hv}\boldsymbol{\omega}^{kl,kj^H}_{hv} & \boldsymbol{\omega}^{kl,kj}_{hv}\xi^{kl,kj^H}_{vh} \\ \boldsymbol{\omega}^{kl,kj^H}_{hv}\xi^{kl,kj}_{vh} & 0 \end{bmatrix}, \bar{\mathbf{l}}_{hh} = \begin{bmatrix} \mathbf{l}_{hh} \\ t_{hh} \end{bmatrix},$$

$\bar{\mathbf{l}}_{vh} = \begin{bmatrix} \mathbf{l}_{vh} \\ t_{vh} \end{bmatrix}$, $\mathbf{L}_{hh} = \bar{\mathbf{l}}_{hh}\bar{\mathbf{l}}^H_{hh}$, $\mathbf{L}_{vh} = \bar{\mathbf{l}}_{vh}\bar{\mathbf{l}}^H_{vh}$, (t_{hv}, t_{hh}) are auxiliary variables, and $\left(o^{k,l}_{\mathbf{L}_{hv}}, o^{k,l}_{\mathbf{L}_{hh}}\right)$ are slack variables $\forall k, l$.

C. Optimal Phase Shifters for Transmit DP Antennas

By obtaining $\mathbf{\Phi}^{pq}$, $p, q \in \{v, h\}$, from (P1.15), (P1.18), (P1.21), and (P1.22) and by the change of variables $\mathbf{f}^H_{k,l}\mathbf{E}^p_k\{(\mathbf{H}^p_{r,k})^H(\mathbf{\Phi}^{pp}\mathbf{G}^p + \mathbf{\Phi}^{pq}\mathbf{G}^q) + (\mathbf{H}^p_{d,k})^H\}\mathbf{U}^p\mathbf{w}_{i,m} = \mathbf{u}^H_p\boldsymbol{\alpha}^{kl,im}_p$, $\mathbf{f}^H_{k,l}\mathbf{E}^p_k\{(\mathbf{H}^p_{r,k})^H(\mathbf{\Phi}^{pp}\mathbf{G}^p + \mathbf{\Phi}^{pq}\mathbf{G}^q) + (\mathbf{H}^p_{d,k})^H\}\mathbf{U}^p\mathbf{w}_{k,j} = \mathbf{u}^H_p\boldsymbol{\alpha}^{kl,kj}_p$, where $\boldsymbol{\alpha}^{kl,im}_p = \text{diag}(\mathbf{f}^H_{k,l}\mathbf{E}^p_k\{(\mathbf{H}^p_{r,k})^H(\mathbf{\Phi}^{pp}\mathbf{G}^p + \mathbf{\Phi}^{qp}\mathbf{G}^q) + (\mathbf{H}^p_{d,k})^H\})\mathbf{w}_{i,m}$, $\boldsymbol{\alpha}^{kl,kj}_p = \text{diag}(\mathbf{f}^H_{k,l}\mathbf{E}^p_k\{(\mathbf{H}^p_{r,k})^H(\mathbf{\Phi}^{pp}\mathbf{G}^p + \mathbf{\Phi}^{qp}\mathbf{G}^q) + (\mathbf{H}^p_{d,k})^H\})\mathbf{w}_{k,j}$, and $\mathbf{u}_p = [e^{-j\gamma_{p,1}}, e^{-j\gamma_{p,2}}, e^{-j\gamma_{p,3}}, \cdots, e^{-j\gamma_{p,N_t}}]^H$, (P1.6) for $\mathbf{U}^v$ and $\mathbf{U}^h$ is reduced to

$$\begin{aligned} &\max_{\mathbf{u}_p} \sum_{k=1}^{K}\sum_{l=1}^{L_k}\log_2\left(1 + \frac{\left|\mathbf{u}^H_v\boldsymbol{\alpha}^{kl,kl}_v + \mathbf{u}^H_h\boldsymbol{\alpha}^{kl,kl}_h\right|^2}{\sum_{i\neq k}^{K}\sum_{m=1}^{L_i}\left|\mathbf{u}^H_v\boldsymbol{\alpha}^{kl,im}_v + \mathbf{u}^H_h\boldsymbol{\alpha}^{kl,im}_h\right|^2 + \sum_{j\neq l}^{L_k}\left|\mathbf{u}^H_v\boldsymbol{\alpha}^{kl,kj}_v + \mathbf{u}^H_h\boldsymbol{\alpha}^{kl,kj}_h\right|^2 + \sigma^2}\right) \\ &\text{s.t. } c_k \geq \lambda_k, \forall k, \ \left|\mathbf{u}_{p_{(n_t)}}\right| = 1, \ n_t = 1, \cdots, N_t, \ p \in \{v, h\}. \end{aligned} \tag{P1.24}$$

Now, we solve (P1.23) separately for $\mathbf{u}_v$ and $\mathbf{u}_h$.

1) Optimization of Transmit Vertical Phase Shifts: Here, we address (P1.15) concerning the vertical phase shifters of the transmit DP antennas. By letting $\mathbf{u}^H_h\boldsymbol{\alpha}^{kl,im}_h = \vartheta^{kl,im}_h$, and $\mathbf{u}^H_h\boldsymbol{\alpha}^{kl,kj}_h = \vartheta^{kl,kj}_h$, where $\mathbf{u}_h = [1, 1, \cdots, 1]^H$, the problem (P1.23) for $\mathbf{u}^v$ can be reduced to

$$\begin{aligned} &\max_{\mathbf{V}_v} \sum_{k=1}^{K}\sum_{l=1}^{L_k}\log_2\left(1 + \frac{\text{trace}\left(\mathbf{A}^{kl,kl}_v\mathbf{V}_v\right) + \left|\vartheta^{kl,kl}_h\right|^2}{\sum_{i\neq k}^{K}\sum_{m=1}^{L_i}\text{trace}\left(\mathbf{A}^{kl,im}_v\mathbf{V}_v\right) + \sum_{j\neq l}^{L_k}\text{trace}\left(\mathbf{A}^{kl,kj}_v\mathbf{V}_v\right) + \left|\vartheta^{kl,kj}_h\right|^2 + \sum_{i\neq k}^{K}\sum_{m=1}^{L_i}\left|\vartheta^{kl,im}_h\right|^2 + \sigma^2}\right) \\ &\text{s.t.} \quad c_k \geq \lambda_k, \forall k, \ \mathbf{V}_v \succeq 0, \ \zeta^{k,l}_v \geq 0, \ \forall k, \\ &\qquad \mathbf{V}_{v_{(n_t,n_t)}} = 1, \ n_t = 1, \cdots, N_t + 1, \end{aligned} \tag{P1.25}$$

where $\mathbf{A}^{kl,im}_v = \begin{bmatrix} \boldsymbol{\alpha}^{kl,im}_v\left(\boldsymbol{\alpha}^{kl,im}_v\right)^H & \boldsymbol{\alpha}^{kl,im}_v\left(\vartheta^{kl,im}_h\right)^H \\ \boldsymbol{\omega}^{kl,im^H}_{vv}\vartheta^{kl,im}_h & 0 \end{bmatrix}$, $\mathbf{A}^{kl,kj}_v = \begin{bmatrix} \boldsymbol{\alpha}^{kl,kj}_v\left(\boldsymbol{\alpha}^{kl,kj}_v\right)^H & \boldsymbol{\alpha}^{kl,kj}_v\left(\vartheta^{kl,kj}_h\right)^H \\ \boldsymbol{\omega}^{kl,kj^H}_{vv}\vartheta^{kl,kj}_h & 0 \end{bmatrix}$, and, $\bar{\mathbf{u}}_v = \begin{bmatrix} \mathbf{u}_v \\ t_v \end{bmatrix}$, and t_v is an auxiliary variable. By applying a series of steps analogous to those used in (P1.11), we can derive the final convex formulation for (P1.25):

$$\begin{aligned} &\max_{\mathbf{V}_v, y_{kl}} \sum_{k=1}^{K} o^k_{\mathbf{V}_v} \\ &\text{s.t.} \quad \text{GM}\left(\mathbf{x}^k_{\mathbf{V}_v}\right) \geq \zeta^k_v + o^k_{\mathbf{V}_v}, \forall k, \\ &\qquad \mathbf{V}_v \succ 0, \quad y_{kl} \in \mathbb{R}, \forall k, l, \\ &\qquad \mathbf{V}_{v(n_t,n_t)} = 1, \quad n_t = 1, \cdots, N_t + 1, \end{aligned} \tag{P1.26}$$

where

$$\mathbf{x}^k_{\mathbf{V}_v} = \left[x^{k,1}_{\mathbf{V}_v}, \cdots, x^{k,L_k}_{\mathbf{V}_v}\right],$$

$$x^{k,l}_{\mathbf{V}_v} = 1 + 2y_{kl}\left(\sqrt{\text{trace}\left(\mathbf{A}^{kl,kl}_v\mathbf{V}_v\right) + \left|\vartheta^{kl,kl}_h\right|^2}\right)$$

$$-y^2_{kl}\left(\sum_{i\neq k}^{K}\sum_{m=1}^{L_i}\text{trace}\left(\mathbf{A}^{kl,im}_v\mathbf{V}_v\right) + \left|\vartheta^{kl,im}_h\right|^2\right)$$

$$-y_{kl}^2\left(\sum_{j\neq l}^{L_k}\text{trace}\left(\mathbf{A}_v^{kl,kj}\mathbf{V}_v\right)+\left|\vartheta_h^{kl,kj}\right|^2\right)+\sigma^2,\forall k,l,$$

and $\zeta_{\mathbf{V}_v}^k$ and $o_{\mathbf{V}_v}^k$ are slack variables and real positive numbers $\forall k$, respectively.

2) Optimization of Transmit Horizontal Phase Shifts: By employing methodologies analogous to those used for $\mathbf{U}^v$, we can derive a convex formulation for $\mathbf{U}^h$ as follows (details are omitted due to space limitations):

$$\begin{aligned}\max_{\mathbf{V_h},y_{kl}}\ &\sum_{k=1}^{K}o_{\mathbf{V}_h}^k\\ \text{s.t.}\quad &\text{GM}\left(\mathbf{x}_{\mathbf{V}_h}^k\right)\geq\zeta_h^k+o_{\mathbf{V}_h}^k,\ \forall k,\\ &\mathbf{V}_h\succ 0,\quad y_{kl}\in\mathbb{R},\ \forall k,l,\\ &\mathbf{V}_{h(n_t,n_t)}=1,\quad n_t=1,\cdots,N_t+1.\end{aligned}\tag{P1.28}$$

where

$$\mathbf{x}_{\mathbf{V}_h}^k=\left[x_{\mathbf{V}_h}^{k,1},\cdots,x_{\mathbf{V}_h}^{k,L_k}\right],$$

$$x_{\mathbf{V}_h}^{k,l}=1+2y_{kl}\left(\sqrt{\text{trace}\left(\mathbf{A}_h^{kl,kl}\mathbf{V}_h\right)+\left|\vartheta_v^{kl,kl}\right|^2}\right)$$

$$-y_{kl}^2\left(\sum_{i\neq k}^{K}\sum_{m=1}^{L_i}\text{trace}\left(\mathbf{A}_h^{kl,im}\mathbf{V}_h\right)+\left|\vartheta_v^{kl,im}\right|^2\right)$$

$$-y_{kl}^2\left(\sum_{j\neq l}^{L_k}\text{trace}\left(\mathbf{A}_h^{kl,kj}\mathbf{V}_h\right)+\left|\vartheta_v^{kl,kj}\right|^2\right)+\sigma^2,\forall k,l,$$

$$\mathbf{A}_h^{kl,im}=\begin{bmatrix}\boldsymbol{\alpha}_h^{kl,im}\left(\boldsymbol{\alpha}_h^{kl,im}\right)^H & \boldsymbol{\alpha}_h^{kl,im}\left(\vartheta_v^{kl,im}\right)^H\\ \left(\boldsymbol{\alpha}_h^{kl,im}\right)^H\vartheta_v^{kl,im} & 0\end{bmatrix},$$

$$\mathbf{A}_h^{kl,kj}=\begin{bmatrix}\boldsymbol{\alpha}_h^{kl,kj}\left(\boldsymbol{\alpha}_h^{kl,kj}\right)^H & \boldsymbol{\alpha}_h^{kl,kj}\left(\vartheta_v^{kl,kj}\right)^H\\ \boldsymbol{\alpha}_h^{kl,kj^H}\vartheta_v^{kl,kj} & 0\end{bmatrix},$$

$\overline{\mathbf{u}}_h=\begin{bmatrix}\mathbf{u}_h\\ t_h\end{bmatrix}$, $(\overline{\mathbf{u}}_h)^H\mathbf{A}_h^{k,i}\overline{\mathbf{u}}_h=\text{trace}\left(\mathbf{A}_h^{k,i}\mathbf{V}_h\right)$, and $\mathbf{V}_h=\overline{\mathbf{u}}_h(\overline{\mathbf{u}}_h)^H,\ \forall k,l$.

D. Optimal Phase Shifters for Receive DP Antennas

Given $\boldsymbol{\Phi}^{pq}$ and $\mathbf{U}^p$, $p,q\in\{v,h\}$, from (P1.15), (P1.18), (P1.21), (P1.22), (P1.26),(P1.28), respectively, following the change of variables $\mathbf{f}_{k,l}^H\mathbf{E}_k^p\{(\mathbf{H}_{r,k}^p)^H(\boldsymbol{\Phi}^{pp}\mathbf{G}^p+\boldsymbol{\Phi}^{qp}\mathbf{G}^q)+(\mathbf{H}_{d,k}^p)^H\}\mathbf{U}^p\mathbf{w}_{i,m}=(\mathbf{e}_p^k)^H\mathbf{h}_p^{'kl,im}$, $\mathbf{f}_{k,l}^H\mathbf{E}_k^p\{(\mathbf{H}_{r,k}^p)^H(\boldsymbol{\Phi}^{pp}\mathbf{G}^p+\boldsymbol{\Phi}^{qp}\mathbf{G}^q)+(\mathbf{H}_{d,k}^p)^H\}\mathbf{U}^p\mathbf{w}_{k,j}=(\mathbf{e}_p^k)^H\mathbf{h}_p^{'kl,kj}$, where $\mathbf{h}_p^{'kl,im}=\text{diag}(\mathbf{f}_k^H)\mathbf{h}_p^{k,i}$, $\mathbf{h}_p^{'kl,kj}=\text{diag}(\mathbf{f}_k^H)\mathbf{h}_p^{kl,kj}$, $\mathbf{h}_p^{kl,im}=(\mathbf{H}_{r,k}^p)^H(\boldsymbol{\Phi}^{pp}\mathbf{G}^p+\boldsymbol{\Phi}^{qp}\mathbf{G}^q)\mathbf{U}^p\mathbf{w}_{i,m}+(\mathbf{H}_{d,k}^p)^H\mathbf{U}^p\mathbf{w}_{i,m}$, and $\mathbf{h}_p^{kl,kj}=(\mathbf{H}_{r,k}^p)^H(\boldsymbol{\Phi}^{pp}\mathbf{G}^p+\boldsymbol{\Phi}^{qp}\mathbf{G}^q)\mathbf{U}^p\mathbf{w}_{k,j}+(\mathbf{H}_{d,k}^p)^H\mathbf{U}^p\mathbf{w}_{k,j}$, and $\mathbf{e}_p^k=[e^{-j\delta_{p,1}},e^{-j\delta_{p,2}},e^{-j\delta_{p,3}},\cdots,e^{-j\delta_{p,N_{r,k}}}]^H$, $p\in\{v,h\},\forall k$, the problem (P1.6) can be reformulated as

$$\begin{aligned}\max_{\mathbf{e}_p^k}\ &\sum_{l=1}^{L_k}\log_2\left(1+\frac{\left|\left(\mathbf{e}_v^k\right)^H\mathbf{h}_v^{'kl,kl}+\left(\mathbf{e}_h^k\right)^H\mathbf{h}_h^{'kl,kl}\right|^2}{\sum_{i\neq k}^{K}\sum_{m=1}^{L_i}\left|\left(\mathbf{e}_v^k\right)^H\mathbf{h}_v^{'kl,im}+\left(\mathbf{e}_h^k\right)^H\mathbf{h}_h^{'kl,im}\right|^2+\sum_{j\neq l}^{L_k}\left|\left(\mathbf{e}_v^k\right)^H\mathbf{h}_v^{'kl,kj}+\left(\mathbf{e}_h^k\right)^H\mathbf{h}_h^{'kl,kj}\right|^2+\sigma^2}\right)\\ \text{s.t.}\quad &c_k\geq\lambda_k,\forall k,\ \mathbf{h}_p^{'k,i}=\text{diag}\left(\mathbf{f}_k^H\right)\mathbf{h}_p^{k,i},\\ &\mathbf{e}_p^k=\left[e^{-j\delta_{p,1}},\cdots,e^{-j\delta_{p,N_{r,k}}}\right]^H,\ p\in\{v,h\},\forall k.\end{aligned}\tag{P1.29}$$

We observe that the optimization of $\mathbf{E}_k^p$ for a specific user k does not impact the performance of other users. As a result, one of the receive phase shifters for all users, either horizontal or vertical, can be held constant, while the other is subject to optimization. By letting $\mathbf{e}_h^k=[e^{-j\delta_{p,1}},e^{-j\delta_{p,2}},e^{-j\delta_{p,3}},\cdots,e^{-j\delta_{p,N_{r,k}}}]^H$, $\forall k$ and defining $\left(\mathbf{e}_h^k\right)^H\mathbf{h}_h^{'k,i}=\chi_h^{k,i}$, $\forall k$, the problem (P1.29) for $\mathbf{e}_v^k$, $\forall k$ can be written as

$$\begin{aligned}\max_{\mathbf{e}_v^k}\ &\sum_{l=1}^{L_k}\log_2\left(1+\frac{\left|\left(\mathbf{e}_v^k\right)^H\mathbf{h}_v^{'kl,kl}+\chi_h^{kl,kl}\right|^2}{\sum_{i\neq k}^{K}\sum_{m=1}^{L_i}\left|\left(\mathbf{e}_v^k\right)^H\mathbf{h}_v^{'kl,im}+\chi_h^{kl,im}\right|^2+\sum_{j\neq l}^{L_k}\left|\left(\mathbf{e}_v^k\right)^H\mathbf{h}_v^{'kl,kj}+\chi_h^{kl,kj}\right|^2+\sigma^2}\right)\\ \text{s.t.}\quad &c_k\geq\lambda_k,\forall k,\ \mathbf{h}_v^{'k,i}=\text{diag}\left(\mathbf{f}_k^H\right)\mathbf{h}_v^{k,i},\ \forall k.\\ &\mathbf{e}_v^k=\left[e^{-j\delta_{v,1}},\cdots,e^{-j\delta_{v,N_{r,k}}}\right]^H,\forall k.\end{aligned}\tag{P1.30}$$

Defining $\mathbf{B}_v^{kl,im}=\begin{bmatrix}\mathbf{h}_v^{'kl,im}\left(\mathbf{h}_v^{'kl,im}\right)^H & \mathbf{h}_v^{'kl,im}\left(\chi_h^{kl,im}\right)^H\\ \left(\mathbf{h}_v^{'kl,im}\right)^H\chi_h^{kl,im} & 0\end{bmatrix}$,

$\mathbf{B}_v^{kl,kj}=\begin{bmatrix}\mathbf{h}_v^{'kl,kj}\left(\mathbf{h}_v^{'kl,kj}\right)^H & \mathbf{h}_v^{'kl,kj}\left(\chi_h^{kl,kj}\right)^H\\ \left(\mathbf{h}_v^{'kl,kj}\right)^H\chi_h^{kl,kj} & 0\end{bmatrix}$,

$\overline{\mathbf{e}}_v^k=\begin{bmatrix}\mathbf{e}_v\\ t_v\end{bmatrix}$, $\left(\overline{\mathbf{e}}_v^k\right)^H\mathbf{B}_v^{kl,im}\overline{\mathbf{e}}_v^k=\text{trace}\left(\mathbf{B}_v^{kl,im}\overline{\mathbf{e}}_v^k\left(\overline{\mathbf{e}}_v^k\right)^H\right)=\text{trace}\left(\mathbf{B}_v^{kl,im}\mathbf{O}_v^k\right)$, $\left(\overline{\mathbf{e}}_v^k\right)^H\mathbf{B}_v^{kl,kj}\overline{\mathbf{e}}_v^k=\text{trace}\left(\mathbf{B}_v^{kl,kj}\overline{\mathbf{e}}_v^k\left(\overline{\mathbf{e}}_v^k\right)^H\right)=\text{trace}\left(\mathbf{B}_v^{kl,kj}\mathbf{O}_v^k\right)$ and relaxing the constraint $\text{rank}\left(\mathbf{O}_v^k\right)=1,\ \forall k$, an equivalent formulation for (P1.30) is given by

$$\begin{aligned}\max_{\mathrm{O}_v^k}\ &\sum_{l=1}^{L_k}\log_2\left(1+\frac{\text{trace}\left(\mathbf{B}_v^{kl,kl}\mathrm{O}_v^k\right)+\left|\chi_h^{kl,kl}\right|^2}{\sum_{i\neq k}^{K}\sum_{m=1}^{L_i}\text{trace}\left(\mathbf{B}_v^{kl,im}\mathrm{O}_v^k\right)+\left|\chi_h^{kl,im}\right|^2+\sum_{j\neq l}^{L_k}\text{trace}\left(\mathbf{B}_v^{kl,kj}\mathrm{O}_v^k\right)+\left|\chi_h^{kl,kj}\right|^2+\sigma^2}\right)\\ \text{s.t.}\quad &c_k\geq\lambda_k,\forall k,\ \mathrm{O}_v^k\succeq 0,\ \forall k,\\ &\mathrm{O}_{v\left(n_{r,k},n_{r,k}\right)}^k=1,\ n_{r,k}=1,\cdots,N_{r,k}+1,\ \forall k.\end{aligned}\tag{P1.31}$$

Utilizing analogous steps as applied to (P1.12), we derive the convex formulation for (P1.31):

$$\begin{aligned}\max_{\mathrm{O}_h^k, y_{kl}} \quad & o^k_{\mathrm{O}_h^k} \\ \text{s.t.} \quad & \mathrm{GM}\left(\mathbf{x}^k_{\mathrm{O}_h^k}\right) \geq \zeta_v^k + o^k_{\mathrm{O}_h^k}, \forall k, \\ & \mathrm{O}_h^k \succ 0,\, y_{kl} \in \mathbb{R}, \forall k, l, \\ & \mathrm{O}^k_{h(n_{r,k}, n_{r,k})} = 1,\, n_{r,k} = 1, \cdots, N_{r,k}+1, \forall k,\end{aligned} \tag{P1.32}$$

where

$$\mathbf{x}^k_{\mathrm{O}_v^k} = \left[x^{k1}_{\mathrm{O}_v^k}, \cdots, x^{kL_k}_{\mathrm{O}_v^k}\right]$$

and

$$x^{kl}_{\mathrm{O}_v^k} = 1 + 2y_{k1}\left(\sqrt{\mathrm{trace}\left(\mathbf{B}_v^{k1,k1}\mathrm{O}_v^k\right) + \left|\chi_h^{k1,k1}\right|^2}\right)$$

$$-y_{k1}^2 \sum_{i\neq k}^{K}\sum_{m=1}^{L_i}\left(\mathrm{trace}\left(\mathbf{B}_v^{k1,im}\mathrm{O}_v^k\right) + \left|\chi_h^{k1,im}\right|^2\right)$$

$$-y_{k1}^2 \sum_{j\neq l}^{L_k}\left(\mathrm{trace}\left(\mathbf{B}_v^{k1,kj}\mathrm{O}_v^k\right) + \left|\chi_h^{k1,kj}\right|^2\right) + \sigma^2, \forall k, l$$

E. Overall Algorithm

The proposed AO algorithm sequentially tackles (P1.1), (P1.16), (P1.19), (P1.22), (P1.23), (P1.26), (P1.28), and (P1.32) until achieving convergence of the objective function defined in (P1). To maintain a monotonically non-increasing behavior, the maximized objective value o^k obtained from each problem serves as the subsequent problem's ζ^k. The complete algorithm is detailed in Algorithm 1.

Algorithm 1 Multi step AO Algorithm for Solving (P1)

1: Set iteration $i = 0$ and initialize $\mathbf{\Phi}_i^{pq} = \mathbf{I}_{\mathbf{\Phi}^{pq}}$, $\mathbf{U}_i^p = \mathbf{I}_{\mathbf{U}^p}$, $\mathbf{E}_{k,i}^p = \mathbf{I}_{\mathbf{E}_{k,i}^p}$, $L_{i,k} = \min(N_t, N_{r,k})$, $\mathbf{W}_i = \frac{1}{\sqrt{N_t}}[\mathbf{1}, \mathbf{1}, \cdots, \mathbf{1}_{1,L_1}, \cdots, \mathbf{1}_{K,L_K}]^T$, $\mathbf{p}_i = \frac{P_{\max}}{\sum_{k=1}^{K}\min(N_t,N_{r,k})}[1, 1, \cdots, 1_{1,L_1}, \cdots, 1_{K,L_K}]$, and $o^k_{\mathbf{O}_v,i} = 0\,\forall k$.
2: **repeat**
3: Given $\mathbf{\Phi}_i^{pq}$, $\mathbf{U}_i^p$, and $\mathbf{E}_{k,i}^p$, $\forall k$, $p, q \in \{v, h\}$, calculate the composite channel $\mathbf{H}_k, \forall k$.
4: **repeat**
5: Given $\mathbf{p}_i$, $L_{i,k}$, and $\mathbf{W}_i$, calculate $\mathbf{F}_{k,i}, \forall k$ using (6).
6: Given $\mathbf{F}_{k,i}, \forall k$, $L_{i,k}, \forall k$, and $\mathbf{p}_i$, update $\mathbf{W}_i$ using (5).
7: Given $\mathbf{F}_{k,i}, \forall k$, $\mathbf{W}_i$, and $\mathbf{p}_i$ solve (P1.5) and update $L_{i,k}$ as $\left[\lambda_{k,1,\cdots}, \lambda_{k,\min(N_t,N_{r,k})}\right] > 0$, $\forall k$.
8: Given $L_{i,k}, \forall k$, $\mathbf{F}_{k,i}, \forall k$, and $\mathbf{W}_i$, update $\mathbf{p}_i$ using (7)
9: **until** the objective value of (P1.1) converges or the maximum number of iterations are completed.
10: Given $\mathbf{U}_i^v$, $\mathbf{U}_i^h$, $\mathbf{\Phi}_i^{hv}$, $\mathbf{\Phi}_i^{vh}$, and $\mathbf{\Phi}_i^{hh}$, set $\zeta^k_{\mathbf{L}_{vv},i} = o^k_{\mathbf{O}_v,i}$, $\forall k$, solve (P1.16), extract $\mathbf{\Phi}_{i+1}^{vv}$ from $\mathbf{L}_{vv}$, and obtain $o^k_{\mathbf{L}_{vv},i}, \forall k, l$. If (P1.16) becomes infeasible, proceed to the next step.
11: Given $\mathbf{\Phi}_{i+1}^{vv}$, set $\zeta^k_{\mathbf{L}_{hv},i} = o^k_{\mathbf{L}_{vv},i}, \forall k$, solve (P1.19), extract $\mathbf{\Phi}_{i+1}^{hv}$ from $\mathbf{L}_{hv}$, and obtain $o^k_{\mathbf{L}_{hv},i}, \forall k, l$. If (P1.19) becomes infeasible, proceed to the next step.
12: Given $\mathbf{\Phi}_{i+1}^{vv}$ and $\mathbf{\Phi}_{i+1}^{hv}$, set $\zeta^k_{\mathbf{L}_{vh},i} = o^k_{\mathbf{L}_{hv},i}$, $\forall k$, solve (P1.23), extract $\mathbf{\Phi}_{i+1}^{vh}$ from $\mathbf{L}_{vh}$, and obtain $o^k_{\mathbf{L}_{vh},i}, \forall k, l$. If (P1.23) becomes infeasible, proceed to the next step.
13: Given $\mathbf{\Phi}_{i+1}^{vh}$, set $\zeta^k_{\mathbf{L}_{hh},i} = o^k_{\mathbf{L}_{vh},i}, \forall k$, solve (P1.22), extract $\mathbf{\Phi}_{i+1}^{hh}$ from $\mathbf{L}_{hh}$, and obtain $o^k_{\mathbf{L}_{hh},i}$, $\forall k, l$. If (P1.22) becomes infeasible, proceed to the next step.
14: Given $\mathbf{\Phi}_{i+1}^{pq}$, $p, q \in \{v, h\}$, set $\zeta^k_{\mathbf{V}_v,i} = o^k_{\mathbf{L}_{hh},i}, \forall k$, solve (P1.26), extract $\mathbf{U}_{i+1}^v$ from $\mathbf{V}_v$, and obtain $o^k_{\mathbf{V}_v,i}, \forall k, l$. If (P1.26) becomes infeasible, proceed to the next step.
15: Given $\mathbf{U}_{i+1}^v$, set $\zeta^k_{\mathbf{V}_h,i} = o^k_{\mathbf{V}_v,i}, \forall k$, solve (P1.28), extract $\mathbf{U}_{i+1}^h$ from $\mathbf{V}_h$, and obtain $o^k_{\mathbf{V}_h,i}, \forall k, l$. If (P1.28) becomes infeasible, proceed to the next step.
16: Given $\mathbf{\Phi}_{i+1}^{pq}$ and $\mathbf{U}_{i+1}^p$, $p, q \in \{v, h\}$, set $\zeta^k_{\mathbf{O}_v,i} = o^k_{\mathbf{V}_h,i}, \forall k$, solve (P1.32), extract $\mathbf{E}_{k,i+1}^v$ from $\mathbf{O}_k^v, \forall k$, and obtain $o^k_{\mathbf{O}_v,i+1}, \forall k, l$. If (P1.32) becomes infeasible, proceed to the next step.
17: Update $i = i + 1$.
18: **until** the objective value of (P1) converges or the maximum number of iterations are completed.

IV. Fixed Weights based Low Complexity Scheme

In this section, we introduce Algorithm 2, designed as a low-complexity alternative to Algorithm 1. More specifically, by anticipating the number of data streams for all users and predefining the corresponding weightage parameters in (P1.5), (P1.16), (P1.19), (P1.22), (P1.23), (P1.26), (P1.28), and (P1.32) before initiating Algorithm 1, a significant reduction in computational cost can be achieved. This reduction stems from a decrease in the number of optimization variables in the mentioned problems. The time complexity, representing the computational cost, is detailed in Table II. The comprehensive algorithm is detailed in Algorithm 2.

A. Complexity Analysis

We provide the analytical complexity analysis of the derived convex formulations and closed-form solutions in terms of floating point operations (FLOPs) and Big-O notation. In (5) and (6), we provide the solutions for $\mathbf{w}_{k,l}$ and $\mathbf{f}_{k,l}$ for all k and l. Note that the matrices in (5) and (6) are rank-1 matrices. Hence, exploiting the Lanczos algorithm to calculate $\mathbf{w}_{k,l}$ and $\mathbf{f}_{k,l}$ filters results in a complexity of $\mathcal{O}(mN_t)$ and $\mathcal{O}(mN_r)$, respectively, where m denotes the number of iterations in the Lanczos algorithm.

Regarding the power allocations (7), we have provided closed solutions, hence exact FLOPs can be easily calculated as: $(2N_{r,k}N_t + 2N_{r,k} + 1) \times \left(\sum_{k=1}^{K} L_k\right)^2 + \left(\sum_{k=1}^{K} L_k\right)^2 + \sum_{k=1}^{K} L_k\left(N_t - 1\right)\sum_{k=1}^{K} L_k N_t$.

Now, we discuss the complexity of the derived convex formulations, i.e., (P1.16), (P1.19), (P1.22), (P1.23), (P1.26),

(P1.28), and (P1.32). Assuming the primal-dual path-following method [33] and without exploiting any sparsity or special structures in the variables involved in our problems, the worst-case computational complexity of (P1.16), (P1.19), (P1.22), and (P1.23), can be expressed as

$$\mathcal{O}\Bigg(\Big(\max\Big\{\Big(\sum_{k=1}^{K}L_k\Big)^2+\sum_{k=1}^{K}L_k,\ N+\sum_{k=1}^{K}L_k\Big\}\Big)^4 \Big(N+\sum_{k=1}^{K}L_k\Big)^{\frac{1}{2}}\log\Big(\frac{1}{\varepsilon}\Big)\Bigg)$$

while the equivalent logSum-based formulations, i.e., (P1.13), can be shown to have a worst-case complexity of

$$\mathcal{O}\Bigg(\log_2\Bigg(\Big(\max\Big\{\Big(\sum_{k=1}^{K}L_k\Big)^2+\sum_{k=1}^{K}L_k,\ N+\sum_{k=1}^{K}L_k\Big\}\Big)^4\Bigg) \Big(N+\sum_{k=1}^{K}L_k\Big)^{\frac{1}{2}}\log\Big(\frac{1}{\varepsilon}\Big)\Bigg)$$

with ε being the solution accuracy. Additionally, note that formulations (P1.26), (P1.28), and (P1.32) share a similar mathematical nature as (P1.16). Hence, the worst-case computational complexity of (P1.26)/(P1.28) and (P1.32) can be derived as

$$\mathcal{O}\Bigg(\Big(\max\Big\{\Big(\sum_{k=1}^{K}L_k\Big)^2+\sum_{k=1}^{K}L_k,\ N_t+\sum_{k=1}^{K}L_k\Big\}\Big)^4 \Big(N_t+\sum_{k=1}^{K}L_k\Big)^{\frac{1}{2}}\log\Big(\frac{1}{\varepsilon}\Big)\Bigg)$$

and

$$\mathcal{O}\Bigg(\Big(\max\Big\{\Big(\sum_{k=1}^{K}L_k\Big)^2+\sum_{k=1}^{K}L_k,\ N_{r,k}+\sum_{k=1}^{K}L_k\Big\}\Big)^4 \Big(N_{r,k}+\sum_{k=1}^{K}L_k\Big)^{\frac{1}{2}}\log\Big(\frac{1}{\varepsilon}\Big)\Bigg)$$

respectively. Note that the complexity orders are obtained by counting the arithmetic operations of the primal-dual path-following method [33]. Please refer to [32]–[34] and the supplementary files for further details.

We now discuss the computational complexity reduction from Algorithm 1 to Algorithm 2, particularly in solving (P1.16), (P1.19), (P1.22), and (P1.23) for the y_{kl} weights. As discussed in Section IV, the reduced computational cost in Algorithm 2 compared to Algorithm 1 is primarily due to the reduced optimization of the weight variables y_{kl} in (P1.16), (P1.19), (P1.22), (P1.23), (P1.26), (P1.28), and (P1.32). Specifically, by removing the $\sum L_k$ number of constraints and the associated $\sum L_k$ number of optimization variables from the complexity expression, we derive the computational complexity of each subproblem that Algorithm 2 solves. For instance, by removing these constraints and optimization variables from the complexity expression for (P1.16), we obtain a worst-case complexity of $\mathcal{O}\left(\max\left\{\left(\sum_{k=1}^{K}L_k\right)^2, N\right\}^4 N^{\frac{1}{2}}\log\left(\frac{1}{\varepsilon}\right)\right)$.

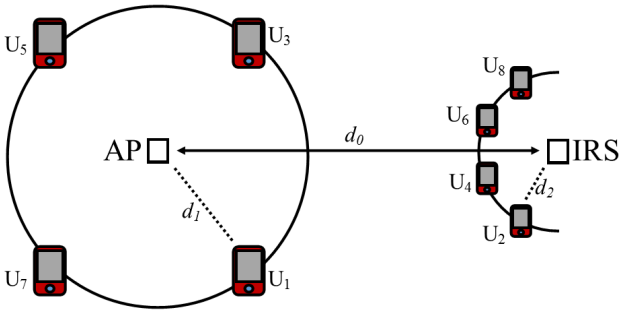

Fig. 2: Simulation setup.

Similarly, the reduced complexity associated with optimizing $\mathbf{U}_p$ and $\mathbf{E}_{p,k}$ can be determined from the aforementioned Big-O expressions by excluding the complexity related to the number of weight optimization variables and corresponding constraints. Consequently, the worst-case complexities to solve $\mathbf{U}_p$ and $\mathbf{E}_{p,k}$ in Algorithm 2 can be expressed as $\mathcal{O}\left(\max\left\{\left(\sum_{k=1}^{K}L_k\right)^2, N_t\right\}^4 N_t^{\frac{1}{2}}\log\left(\frac{1}{\varepsilon}\right)\right)$ and $\mathcal{O}\left(\max\left\{\left(\sum_{k=1}^{K}L_k\right)^2, N_{r,k}\right\}^4 N_{r,k}^{\frac{1}{2}}\log\left(\frac{1}{\varepsilon}\right)\right)$, respectively.

Algorithm 2 Low complexity Algorithm for Solving (P1)

1: Set iteration $i=0$ and initialize $\mathbf{\Phi}_i^{pq}=\mathbf{I}_{\mathbf{\Phi}^{pq}}$, $\mathbf{U}_i^p=\mathbf{I}_{\mathbf{U}^p}$, $\mathbf{E}_{k,i}^p=\mathbf{I}_{\mathbf{E}_{k,i}^p}$, $L_{i,k}$, $\mathbf{W}_i=\frac{1}{\sqrt{N_t}}[\mathbf{1},\mathbf{1},\cdots,\mathbf{1}_{1,L_1},\cdots,\mathbf{1}_{K,L_K}]^T$, $\mathbf{p}_i=\frac{P_{\max}}{\sum_{k=1}^{K}\min(N_t,N_{r,k})}[1,1,\cdots,1_{1,L_1},\cdots,1_{K,L_K}]$, and $o^k_{\mathbf{O}_v,i}=0\,\forall k$.
2: **repeat**
3: Step 3 of Algorithm 1.
4: **repeat**
5: Steps 5, 6, and 8 of Algorithm 1 with fixed $\lambda_{k,l}$, $\forall k,l$.
6: **until** the objective value of (P1.1) converges or the maximum number of iterations are completed.
7: Perform steps 10, 11, 12, 13, 14, 15, and 16 of Algorithm 1 with fix $y_{k,l}$, $\forall k,l$.
8: Update $i=i+1$.
9: **until** the objective value of (P1) converges or the maximum number of iterations are completed.

V. Numerical Analysis and Discussion

A. Simulation Setup

The simulation setup commonly employed for the multi-user scenario is depicted in Fig. 2, wherein eight users, denoted as U_k with $k=1,2,\cdots,8$, are considered. Among them, users U_k with $k=2,4,6,8$ are uniformly distributed along a semi-circle centered around the IRS at a radius of $d_2=3$ m, commonly referred to as "cell-edge" users. Conversely, users U_k with $k=1,3,5,7$ are uniformly distributed along a circle centered around the AP with a radius of $d_2=20$

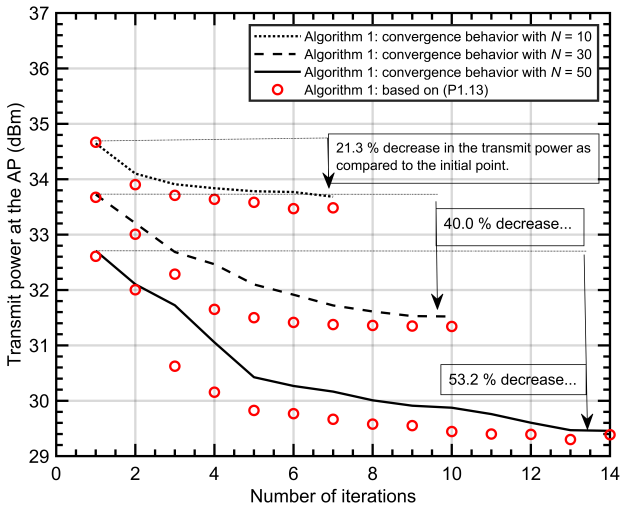

Fig. 3: Convergence behavior of Algorithm 1 with $N = 10, 30,$ and 50.

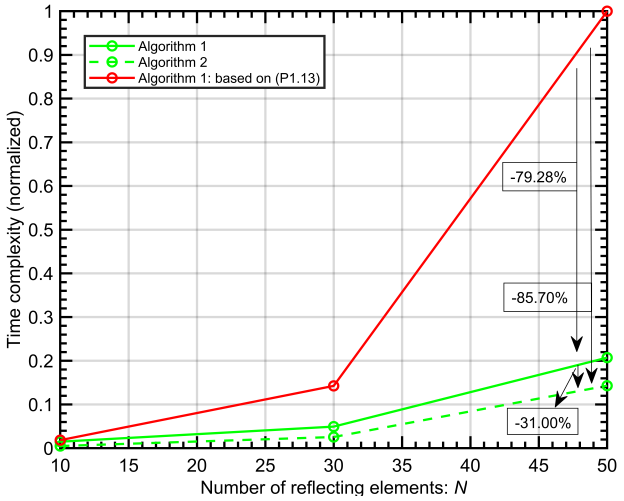

Fig. 4: Normalized time complexity versus the number of reflecting elements.

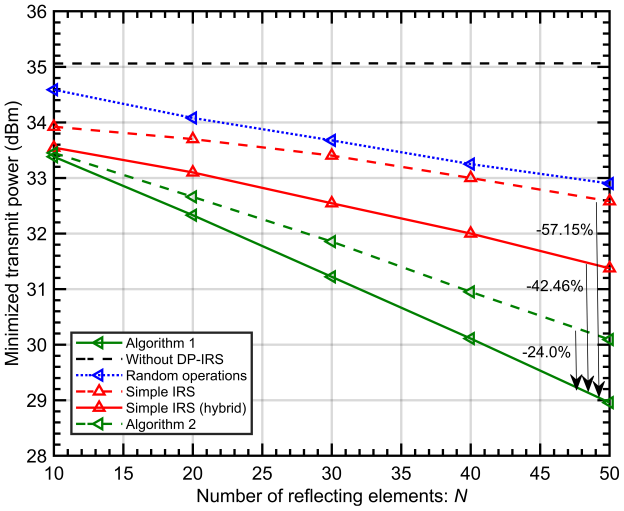

Fig. 5: Minimized transmit power versus the number of reflecting elements.

m. Unless specified otherwise, the simulation parameters are as follows: the distance (d_0) is fixed at 40 m, the path loss exponent a is set to 2.2, 3.2, and 2.8 for the AP-IRS, AP-User, and IRS-User links, respectively. The amplitude of each reflecting element of the DP-IRS is normalized by a factor of $\frac{1}{\sqrt{2}}$, i.e., $\frac{1}{\sqrt{2}}\mathbf{\Psi}$. The path loss ($C_o$) at a reference distance of 1 m, i.e., (D_o), is 30dB. The spectral efficiency λ_k is set to $2(\text{bps/Hz}), \forall k$. Rician fading is applied to the AP-IRS link with a Rician factor (i.e., χ) of $-20, \text{dB}$. The noise power σ_k^2 is $-94\text{dBm}, \forall k$, $N_{r,k}$ is set to 4, $\forall k$, N_t is 16. [2]. In Algorithm 2, $\lambda_{k,l}$ for all l of a user k are selected proportional to the initial normalized SEs. Algorithms terminate if the transmit power reduction in an iteration becomes less than 10^{-3} watts or after a maximum of 15 iterations. The simulation results presented in this study are averaged over 100 channel realizations and computed using MATLAB R2022a on an AMD Ryzen R7-5800H CPU @3.20GHz and 16 GB of RAM.

B. Simulation Results

We commence our discussion by examining the convergence behavior of the proposed algorithm. In Fig. 3, we present the convergence profiles of Algorithm 1 with logsum and GM-based formulations across different values of N. Notably, it is evident that Algorithm 1, utilizing both formulations, converges to nearly identical performance levels and requires a similar number of iterations. Specifically, for N values of 10, 30, and 50, Algorithm 1 reaches convergence in a maximum of 7, 10, and 14 iterations, respectively, resulting in transmit power reductions of 21.3%, 40%, and 53.2% compared to the initial point.

In Fig. 3, despite the comparable performance of Algorithm 1 based on (P1.13) and (P1.16) (logsum[3] and GM-based formulations, respectively), it is noteworthy that the computational cost of logsum expressions is considerably high. Specifically, Table II provides a detailed breakdown of the time complexity of Algorithm 1 based on logsum/GM formulations and Algorithm 2. To enhance interpretability, we present the normalized time complexity in Fig. 4. For instance, when $N = 50$ and $N_t = 16$, it is observed that Algorithm 1, based on the GM-based formulation, and Algorithm 2 require 79% and 85% less computational cost, respectively than Algorithm 1 with logsum-based formulations. Additional insights into the time complexity are available in Table II.

Regarding the optimality of the proposed solutions, while (5), (6), (P1.5), and (7) provide optimal solutions for $\mathbf{W}$, $\mathbf{F}_k$, L_k, and p_k, respectively, the eigenvalue distribution of L in (P1.16) shows that the retrieved $\mathbf{\Phi}$ in the strongest eigen direction of L provides, on average, 61.8%, 58.2%, and 54.6% of the optimal objective value of problem (P1.16), for N = 10, 30, and 50, respectively. More specifically, the lower bounds on the optimality are calculated by dividing the eigenvalue of the strongest eigen direction by the sum of all available eigenvalues [35].

[2]Additional details on simulation setup/parameters and channel models are available in [24], omitted here for brevity

[3]Here, for comparison, an updated formulation of (P1.13) is used, such that it shares the same convergence structure as (P1.16), with only the logsum and GM difference.

In Fig. 5, we present the performance of the proposed algorithms against the number of reflecting elements for various benchmark schemes. The compared schemes are as follows:

Algorithm 1: As observed in Fig. 5, Algorithm 1 results in the lowest transmit power due to the optimized operations at DP-IRS, active/passive beamforming, and vertical/horizontal transmit/receive phase shifters.

Without DP-IRS: In the absence of an IRS in the network, the optimization of $\mathbf{W}$, $\mathbf{F}_k$, L_k, and p_k is carried out using (5), (6), (P1.5), and (7). The absence of IRS results in a significant escalation in the minimum transmit power required at the AP, reaching approximately 35 dBm. This increase in power primarily arises from the presence of cell-edge users, denoted as U_k's, where $k = 2, 4, 6, 8$.

Random Operations: Implementing random operations for DP-IRS leads to enhanced performance compared to the "Without DP-IRS" scenario.

Simple IRS: In this configuration, an S-IRS supports the multiuser MIMO wireless network. The results underscore that DP-IRS requires significantly less transmit power than S-IRS, thanks to its improved inter-layer multiplexing and polarization diversity gains. Furthermore, the performance disparity between the two systems amplifies with an increase in the number of reflecting elements. For instance, DP-IRS with Algorithm 1 necessitates 57.1% less transmit power than S-IRS for 50 reflecting elements.

Simple IRS (hybrid): To establish a more favorable comparison, we examine a scenario where S-IRS aids a wireless network equipped with hybrid antennas at the AP and users (N_t and $N_{r,k}$, respectively) to emulate gains comparable to DP antennas. The results demonstrate that S-IRS with hybrid transmit/receive antennas outperforms S-IRS with simple transmit/receive antennas. However, the proposed Algorithm 1 with DP-IRS surpasses the performance of the hybrid S-IRS-assisted network. For instance, DP-IRS with Algorithm 1 necessitates 42.4% less transmit power than the hybrid S-IRS system for 50 reflecting elements.

Algorithm 2: The results indicate that Algorithm 2 incurs significantly lower computational costs than Algorithm 1 albeit with a trade-off in performance. For instance, as detailed in Table II, Algorithm 2 requires 62.8% less computational time than Algorithm 1 for $N = 10$ and $N_t = 16$. Importantly, the computational complexity gap between Algorithm 1 and Algorithm 2 diminishes with increasing values of N or N_t. This reduction is attributed to the fact that the computational cost associated with N and N_t is substantially higher than their scalar weightage. Consequently, as N and N_t increase, the computational cost gap between Algorithms 1 and 2 decreases. Specifically, as illustrated in Table II and Fig. 4, the computational cost gap decreases from 62.8% when $N = 10$ to 48.2% and 31.0% when N increases to 30 and 50, respectively. Despite this diminishing gap, Algorithm 2 continues to require significantly less computational time while delivering satisfactory performance. Further computational times for various N_t and N values are detailed in Table II. [4]

[4]A detailed analytical computational complexity analysis is provided in the supplementary file for review purposes.

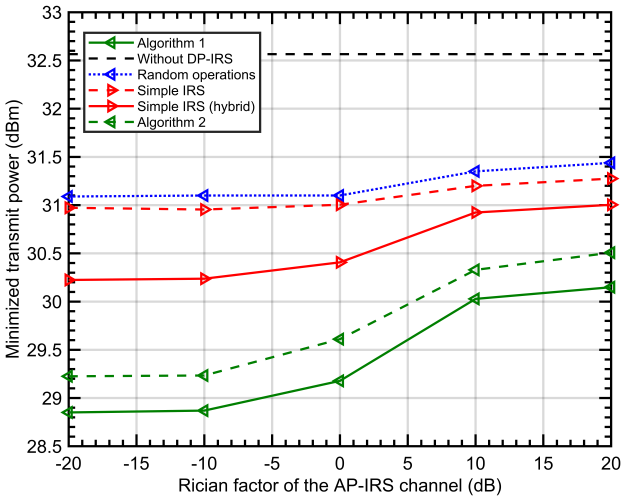

Fig. 6: Minimized transmit power versus the Rician factor of AP-IRS link.

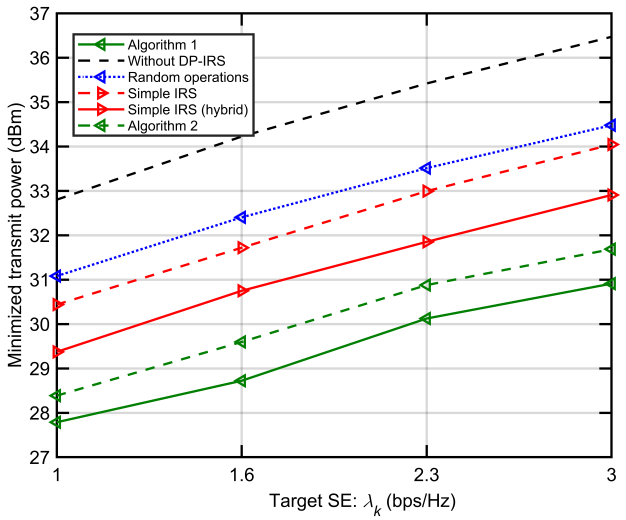

Fig. 7: Minimized transmit power versus the target spectral efficiency.

Mounting the IRS in a wireless network constitutes a variable decision, potentially resulting in a diverse channel type between the transmitter and the IRS. Therefore, exploring the impact of the AP-IRS channel on the proposed system model's performance becomes crucial. Specifically, in Fig. 6, we change the Rician factor of the AP-IRS link, ranging from -20 dB to 20 dB, and illustrate the corresponding minimized transmit power required to achieve specified target performances. Notably, as the Rician factor increases, indicating a line of sight (LoS) environment, the minimum power needed for the target performance rises. Conversely, lower Rician factors, indicative of a non-LoS-rich scattered environment, result in enhanced multiplexing gains, reducing the minimum transmit power. This observation is particularly significant for schemes with hybrid transmit/receive antennas, such as Algorithm 1, Algorithm 2, and Simple IRS (hybrid), as these schemes, with a large number of radiation patches, are more responsive to variations in Rician values. It also suggests that DP-IRS is advantageous over S-IRS when deployed in a non-LoS-rich scattered environment.

This article has been accepted for publication in IEEE Transactions on Wireless Communications. This is the author's version which has not been fully edited and content may change prior to final publication. Citation information: DOI 10.1109/TWC.2025.3567938

TABLE II: Average CPU running time for Algorithms 1 and 2.

	Algorithm 1			Algorithm 2			Algorithm 1: based on (P1.13)		
	$N = 10$	$N = 30$	$N = 50$	$N = 10$	$N = 30$	$N = 50$	$N = 10$	$N = 30$	$N = 50$
$N_t = 16$	28 s	92 s	389 s	10 s	46 s	268 s	34 s	267 s	1878 s
$N_t = 32$	32 s	97 s	421 s	13 s	50 s	280 s	64 s	560 s	3512 s
$N_t = 64$	46 s	113 s	467 s	19 s	60 s	303 s	108 s	976 s	5356 s

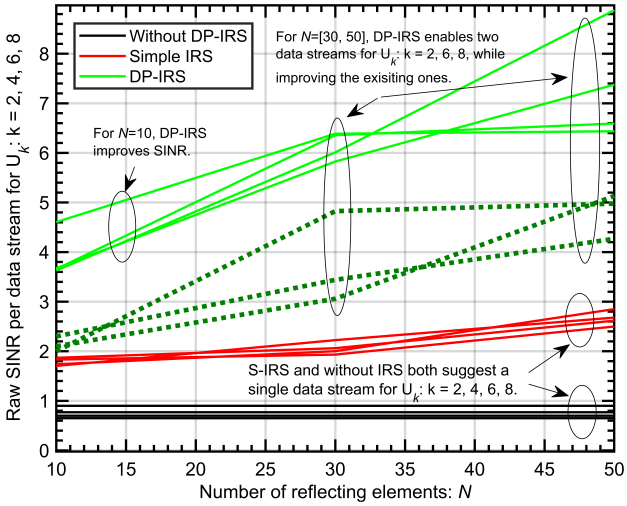

Fig. 8: Inter-layer multiplexing gains versus N for U_k = 2, 4, 6, and 8.

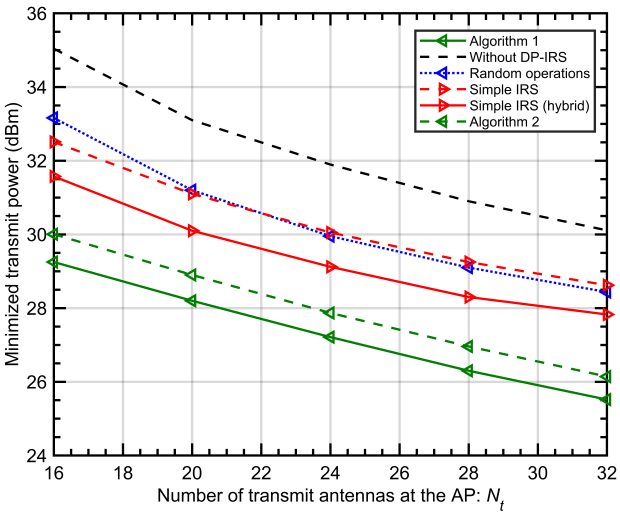

Fig. 10: Minimized transmit power versus the number of transmit antennas.

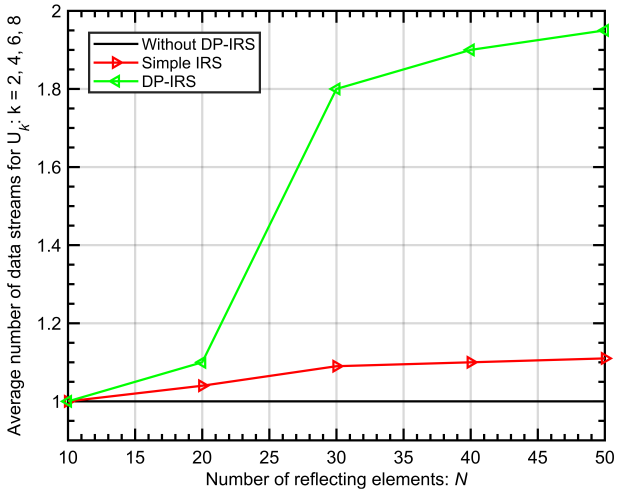

Fig. 9: Average number of data streams versus N for U_k = 2, 4, 6, and 8.

To explicitly observe the interlayer multiplexing gains, Fig. 8 illustrates the raw SINR, i.e., SINR without power allocations, per data stream per user against the number of reflecting elements. Due to the multiplicative fading nature of IRS systems, only U_k = 2, 4, 6, and 8 are considered in Fig. 8. In this figure, it is observed that for $N = 30$ and 50, DP-IRS is capable of multiplexing two data streams for U_k = 2, 4, and 8. Conversely, for $N = 10$, DP-IRS, similar to S-IRS, suggests a single data stream for these users. However, DP-IRS mitigates interference better and improves the performance of the sole available data stream. Similar insights can be observed in Fig. 9.

In Fig. 7, we present the minimized transmit power across different target spectral efficiencies. Doubling the target SE leads to an approximate 1.5 dB increase in transmit power for both Algorithm 1 and Algorithm 2. The performance differences among the compared schemes remain consistent with the previously discussed observations.

Furthermore, Fig. 10 illustrates the minimized transmit power concerning the number of transmit antennas. Doubling the number of transmit antennas, from 16 to 32, results in roughly a 4 dB reduction in transmit power for Algorithm 1 and Algorithm 2. Interestingly, the impact of doubling transmit antennas is more pronounced in schemes with lower performance. This is attributed to the fact that schemes with superior performance are already in power-limited regimes, diminishing the impact of increased transmit antennas. Overall, Algorithms 1 and 2 consistently exhibit the best performance, and the relative differences among the schemes remain as discussed earlier.

VI. Conclusion

In this paper, we investigate the dual-polarized IRS-assisted generalized multiuser MIMO wireless network, allowing for multiple and different numbers of data streams for each user. To harness implicit multiplexing gains, the transmit/receive DP antennas are equipped with single RF chains and separate phase shifters. Within the considered generalized system model, we optimize the number of data streams for each user to achieve the pre-specified target SE with the minimum transit power at the AP. Solving this optimization problem involves optimizing transmit/receive digital filters, power allocations, number of data streams, DP-IRS operations, and transmit/receive vertical/horizontal phase shifters at DP antennas.

For these subproblems, we derive low-complexity convex formulations and propose a novel multistep Algorithm 1 that systematically solves derived formulations, exploits solutions from the previous step, and guarantees convergence to a feasible solution. Additionally, we introduce Algorithm 2, a low-complexity version of Algorithm 1, which exhibits 62.8 % lower computational cost while providing satisfactory performance. Extensive simulation results validate the effectiveness of the proposed algorithms and demonstrate the performance improvements of DP-IRS over S-IRS. Specifically, Algorithm 1 requires 7, 10, and 14 iterations for convergence with 10, 30, and 50 reflecting elements, respectively. Notably, for $N = 50$, DP IRS requires 42.4 % lower transmit power than S-IRS. We also discuss the extension of this work to address the problem of sum capacity maximization and provide a detailed complexity analysis.

The integration of dual-polarization and IRS technologies opens new opportunities for channel estimation techniques, such as joint estimation of the channel for both polarizations and the application of machine learning algorithms. Furthermore, considering specific channel characteristics (e.g., pure LoS or high/low SNR regimes), it is possible to derive low-complexity semi-closed form solutions to (P1). These avenues present interesting future directions for research and will be considered in our future work.

REFERENCES

[1] J. Y. Dai, W. Tang, M. Z. Chen, C. H. Chan, Q. Cheng, S. Jin, and T. J. Cui, "Wireless Communication Based on Information Metasurfaces," *IEEE Trans. Microw. Theory Techn.*, vol. 69, no. 3, pp. 1493–1510, 2021.

[2] E. Basar, M. Di Renzo, J. De Rosny, M. Debbah, M.-S. Alouini, and R. Zhang, "Wireless communications through reconfigurable intelligent surfaces," *IEEE access*, vol. 7, pp. 116 753–116 773, 2019.

[3] S. Abeywickrama, R. Zhang, Q. Wu, and C. Yuen, "Intelligent reflecting surface: Practical phase shift model and beamforming optimization," *IEEE Trans. Commun.*, vol. 68, no. 9, pp. 5849–5863, 2020.

[4] Q. Wu and R. Zhang, "Intelligent reflecting surface enhanced wireless network via joint active and passive beamforming," *IEEE Trans. Wireless Commun.*, vol. 18, no. 11, pp. 5394–5409, 2019.

[5] K. Feng, X. Li, Y. Han, S. Jin, and Y. Chen, "Physical layer security enhancement exploiting intelligent reflecting surface," *IEEE Commun. Lett.*, vol. 25, no. 3, pp. 734–738, 2020.

[6] Y. Jia, C. Ye, and Y. Cui, "Analysis and optimization of an intelligent reflecting surface-assisted system with interference," *IEEE Trans. Wireless Commun.*, vol. 19, no. 12, pp. 8068–8082, 2020.

[7] S. Lin, B. Zheng, G. C. Alexandropoulos, M. Wen, M. Di Renzo, and F. Chen, "Reconfigurable intelligent surfaces with reflection pattern modulation: Beamforming design and performance analysis," *IEEE Trans. Wireless Commun.*, vol. 20, no. 2, pp. 741–754, 2020.

[8] M. Munawar and K. Lee, "Low-Complexity Adaptive Selection Beamforming for IRS-Assisted Single-User Wireless Networks," *IEEE Trans. Veh. Technol.*, vol. 72, no. 4, pp. 5458–5462, 2023.

[9] B. Zheng, C. You, W. Mei, and R. Zhang, "A survey on channel estimation and practical passive beamforming design for intelligent reflecting surface aided wireless communications," *IEEE Commun. Surv. Tutor.*, vol. 24, no. 2, pp. 1035–1071, 2022.

[10] H. Guo and V. K. Lau, "Uplink cascaded channel estimation for intelligent reflecting surface assisted multiuser MISO systems," *IEEE Trans. Signal Process.*, vol. 70, pp. 3964–3977, 2022.

[11] Y. Liu, X. Mu, J. Xu, R. Schober, Y. Hao, H. V. Poor, and L. Hanzo, "STAR: Simultaneous Transmission and Reflection for 360° Coverage by Intelligent Surfaces," *IEEE Wireless Commun.*, vol. 28, no. 6, pp. 102–109, 2021.

[12] H. Zhang and B. Di, "Intelligent Omni-Surfaces: Simultaneous Refraction and Reflection for Full-Dimensional Wireless Communications," *IEEE Commun. Surv. Tutor.*, vol. 24, no. 4, pp. 1997–2028, 2022.

[13] Y. Gao, Q. Wu, G. Zhang, W. Chen, D. W. K. Ng, and M. D. Renzo, "Beamforming Optimization for Active Intelligent Reflecting Surface-Aided SWIPT," *IEEE Trans. Wireless Commun.*, vol. 22, no. 1, pp. 362–378, 2023.

[14] S. Gong, X. Lu, D. T. Hoang, D. Niyato, L. Shu, D. I. Kim, and Y.-C. Liang, "Toward smart wireless communications via intelligent reflecting surfaces: A contemporary survey," *IEEE Commun. Surv. Tutor.*, vol. 22, no. 4, pp. 2283–2314, 2020.

[15] S. Sun, W. Jiang, S. Gong, and T. Hong, "Reconfigurable linear-to-linear polarization conversion metasurface based on PIN diodes," *IEEE Antennas Wirel. Propag. Lett.*, vol. 17, no. 9, pp. 1722–1726, 2018.

[16] J. Wang, R. Yang, R. Ma, J. Tian, and W. Zhang, "Reconfigurable multifunctional metasurface for broadband polarization conversion and perfect absorption," *IEEE Access*, vol. 8, pp. 105 815–105 823, 2020.

[17] H. F. Ma, G. Z. Wang, G. S. Kong, and T. J. Cui, "Independent controls of differently-polarized reflected waves by anisotropic metasurfaces," *Sci. Rep.*, vol. 5, no. 1, p. 9605, 2015.

[18] X. Chen, J. C. Ke, W. Tang, M. Z. Chen, J. Y. Dai, E. Basar, S. Jin, Q. Cheng, and T. J. Cui, "Design and implementation of MIMO transmission based on dual-polarized reconfigurable intelligent surface," *IEEE Wirel. Commun. Lett.*, vol. 10, no. 10, pp. 2155–2159, 2021.

[19] P. Ramezani, M. A. Girnyk, and E. Björnson, "Dual-polarized reconfigurable intelligent surface assisted broad beamforming," *IEEE Commun. Lett.*, 2023.

[20] Y. Han, X. Li, W. Tang, S. Jin, Q. Cheng, and T. J. Cui, "Dual-polarized RIS-assisted mobile communications," *IEEE Trans. Wireless Commun.*, vol. 21, no. 1, pp. 591–606, 2021.

[21] A. Bhowal and S. Aïssa, "MIMO device-to-device communications via cooperative dual-polarized intelligent surfaces," *IEEE Wirel. Commun. Lett.*, vol. 12, no. 2, pp. 202–206, 2022.

[22] S. Sugiura, Y. Kawai, T. Matsui, T. Lee, and H. Iizuka, "Joint beam and polarization forming of intelligent reflecting surfaces for wireless communications," *IEEE Trans. Veh. Technol.*, vol. 70, no. 2, pp. 1648–1657, 2021.

[23] A. S. de Sena, P. H. Nardelli, D. B. da Costa, U. S. Dias, P. Popovski, and C. B. Papadias, "Dual-polarized IRSs in uplink MIMO-NOMA networks: An interference mitigation approach," *IEEE Wirel. Commun. Lett.*, vol. 10, no. 10, pp. 2284–2288, 2021.

[24] M. Munawar and K. Lee, "Dual-Polarized IRS-Assisted MIMO Network," *IEEE Trans. Wireless Commun.*, pp. 1–1, 2023.

[25] A. S. de Sena, P. H. Nardelli, D. B. da Costa, F. R. M. Lima, L. Yang, P. Popovski, Z. Ding, and C. B. Papadias, "IRS-assisted massive MIMO-NOMA networks: Exploiting wave polarization," *IEEE Trans. Wirel. Commun.*, vol. 20, no. 11, pp. 7166–7183, 2021.

[26] M. Munawar and K. Lee, "Dual-polarized IRS-assisted wireless network: relative phase modulation," *EURASIP Journal Wireless Commun. Net.*, vol. 2024, no. 1, p. 22, 2024.

[27] H. Arai, K. Abe, N. Takemura, and T. Mitsui, "Dual-polarized switched beam antenna with variable phase shifter," in *Proc. Int. Workshop on Antenna Technol. (iWAT)*, 2013, pp. 19–22.

[28] B. Clerckx and C. Oestges, *MIMO Wireless Networks: Channels, Techniques and Standards for Multi-Antenna, Multi-User and Multi-Cell Systems*, New York, NY, USA:Academic, 2013.

[29] K. Shen and W. Yu, "Fractional Programming for Communication Systems—Part i: Power Control and Beamforming," *IEEE Trans. Signal Process.*, vol. 66, no. 10, pp. 2616–2630, 2018.

[30] M. Grant and S. Boyd, "CVX: Advanced topics," [online] Available: http://web.cvxr.com/cvx/beta/doc/advanced.html, accessed: August 14, 2022.

[31] ——, "CVX: Matlab Software for Disciplined Convex Programming," [online] Available: http://cvxr.com/cvx, accessed: August 14, 2022.

[32] Z.-q. Luo, W.-k. Ma, A. M.-c. So, Y. Ye, and S. Zhang, "Semidefinite Relaxation of Quadratic Optimization Problems," *IEEE Signal Process. Mag.*, vol. 27, no. 3, pp. 20–34, 2010.

[33] C. Helmberg, F. Rendl, R. J. Vanderbei, and H. Wolkowicz, "An interior-point method for semidefinite programming," *SIAM J. optim.*, vol. 6, no. 2, pp. 342–361, 1996.

[34] W.-K. Ma, C.-C. Su, J. Jaldén, and C.-Y. Chi, "Some results on 16-QAM MIMO detection using semidefinite relaxation," in *IEEE Int. Conf. Acoust. Speech Signal Process.*, 2008, pp. 2673–2676.

[35] Z. Luo, W. Ma, A. M. So, Y. Ye, and S. Zhang, "Semidefinite relaxation of quadratic optimization problems," *IEEE Signal Process. Maga.*, vol. 27, no. 3, pp. 20–34, 2010.